Jokin Echezarreta Pérez

# Tidal channel hydrodynamics and salt marsh deposition under varying sea-level rise scenarios

**Universidade do Algarve**

Faculdade de Ciências e Tecnologia

2020

Jokin Echezarreta Pérez

# Tidal channel hydrodynamics and salt marsh deposition under varying sea-level rise scenarios

**Master in Marine and Coastal Systems**

Work performed under the supervision of:

Ana Rita Carrasco

(Post-Doc Researcher – CIMA, Universidade do Algarve)

Óscar Ferreira

(Post-Doc Researcher – Associate teacher, Universidade do Algarve)

**Universidade do Algarve**

Faculdade de Ciências e Tecnologia

2020

# Tidal channel hydrodynamics and salt marsh deposition under varying sea-level rise scenarios

**Declaração de autoria de trabalho**

Declaro ser o autor deste trabalho, que é original e inédito. Autores e trabalhos consultados estão devidamente citados no texto e constam da listagem de referências incluída.

I declare to be the author of this work, which is original and unpublished. Authors and works consulted are duly cited in the text and are included in the list of references.

Faro, 9 de Outubro de 2020

_____

Jokin Echezarreta Pérez

# ACKNOWLEDGEMENTS

I want to thank my supervisors, Ana Rita Carrasco and Óscar Ferreira, for all their support and patience over the last four years. I want to thank all my friends from the Masters, who are now all over the world and that I will hopefully be joining soon as a Master in Science graduate. A huge thanks to my friend Figo, who helped me immensely to deliver this thesis.

I also want to thank my parents for the inconditional support and love that they have shown me over my stay in Faro, and I hope I earn more of that love going forward. Os quiero mucho aitas.

And finally, I want to thank the main person why I was able to finish: my girlfriend, Patrícia. I wouldn't have been able to do it without you and I can't wait to see what our next chapter brings. Amo-te linda.

# ABSTRACT

In this study, two process-based modelling approaches built in the Delft3D domain were applied to predict changes induced by sea-level rise (SLR) in the tidal circulation and bathymetric evolution of the Ria Formosa coastal lagoon. An unstructured grid modelling approach was calibrated and validated to predict changes in the tidal circulation in the year 2100 of the western sector of the lagoon. The model was forced by tides and a static sea level, with four scenarios of sea-level rise considered. To predict bathymetric changes in the lagoon, a structured grid modelling approach was forced by tides and a linear sea-level rise, with one scenario of sea-level rise considered.

Model results indicate that sea-level rise (SLR) will change residual sediment circulation patterns over the 89-year study period, with the intensity of the impact directly influenced by the intensity of SLR. Under sea-level rise, flood-dominance of the Ancão Inlet increases, hinting to an attenuation of flood dominance in the Faro-Olhão Inlet and a higher role of the Ancão Inlet in capturing the tidal prism. Bathymetric changes over time are considerable in the Ancão and Faro-Olhão inlets and marginal in the channel and tidal marsh areas. Despite some limitations, the results of this study contribute to the scientific knowledge about the impacts of SLR in the hydrodynamics and morphodynamics of coastal lagoons. This study also provides a first exploration of the morphological changes induced by SLR in the Ria Formosa coastal lagoon and recommendations for future research.



Keywords: Ria Formosa; sea-level rise; tidal circulation; bathymetric evolution; long-term

# RESUMO

Neste estudo duas abordagens de modelação baseada em processos (construídas no domínio Delft3D) foram aplicadas para prever mudanças induzidas pela subida do nível do mar na circulação das marés e evolução batimétrica da lagoa costeira da Ria Formosa. Uma abordagem de modelação de malha não estruturada foi calibrada e validada para prever mudanças na circulação das marés no ano 2100 no setor oeste da lagoa. O modelo foi forçado pelas marés e um nível do mar estático, com quatro cenários de subida do nível do mar considerados. Para prever mudanças batimétricas na lagoa, uma abordagem de modelação de malha estruturada foi forçada pelas marés e uma elevação linear do nível do mar, com um cenário de subida do nível do mar considerado.

Os resultados do modelo indicam que a subida do nível do mar (SNM) mudará os padrões da circulação residual de sedimentos ao longo do período de estudo de 89 anos, com a intensidade do impacto diretamente influenciado pela intensidade da SNM. Sob o aumento do nível do mar a dominância de enchente da Barra do Ancão aumenta, sugerindo uma atenuação da dominância de enchente na Barra de Faro-Olhão e um maior protagonismo da Barra do Ancão na captura do prisma das marés. As alterações batimétricas ao longo do tempo são consideráveis nas barras do Ancão e Faro-Olhão e marginais nas zonas do canal e sapal.

Apesar de algumas limitações, os resultados deste estudo contribuem para o conhecimento científico sobre os impactos da SNM na hidrodinâmica e morfodinâmica de lagoas costeiras. Este estudo também fornece uma primeira exploração das alterações morfológicas induzidas por SNM na lagoa costeira da Ria Formosa e recomendações para pesquisas futuras.

Palavras-chave: Ria Formosa; Subida do nível do mar; circulação de maré; evolução batimétrica; longo-termo.

# GENERAL INDEX

# LIST OF FIGURES

# LIST OF TABLES

# LIST OF ABBREVIATIONS

| | |
|---|---|
| ADP | Acoustic Doppler Profiler |
| ADCP | Acoustic Doppler Current Profiler |
| CIMA | Centro de investigação marinha e ambiental |
| COALA | COpernicus for sustainable Agriculture in Australia |
| MORFAC | Morphological acceleration factor |
| RMSE | Root Mean Square Error |
| RSLR | Relative Sea-Level Rise |
| SCORE | Supporting Consumer Ownership in Renewable Energies |
| SLR | Sea-Level Rise |
| SNM | Subida do Nível do Mar |

# Sumário

As lagoas costeiras são áreas altamente produtivas que cobrem cerca de 13% da costa global e fornecem valor na económico e ecológico para as comunidades locais. As lagoas costeiras são particularmente suscetíveis aos impactos induzidos pela subida do nível do mar, como mudanças na hidrodinâmica local, padrões de inundação alterados e perda de áreas húmidas costeiras, entre outros. Devido a esta vulnerabilidade, é vital aumentar o conhecimento sobre a resiliência das lagoas costeiras sob a força da subida do nível do nível do mar (SNM) e melhorar a compreensão dos impactos diretos e indiretos da subida do nível do mar nos regimes hidrodinâmicos e morfológicos de longo prazo das lagoas costeiras. Os principais objetivos deste estudo são analisar os impactos a longo prazo da SNM na circulação da água e na evolução batimétrica da lagoa costeira da Ria Formosa, melhorar o conhecimento existente sobre a dinâmica costeira da Ria Formosa e contribuir para o conhecimento geral sobre a resiliência de lagoas costeiras sob cenários de subida do nível do mar.

Duas abordagens de modelação baseada em processos construídas em Delft3D foram utilizadas neste estudo: uma abordagem de modelação de malha não estruturada (construída por Carrasco et al., 2018) e uma abordagem de modelação de malha estruturada (construída por González-Gorbeña et al., 2018). O modelo de malha não estruturada foi calibrado usando os parâmetros rugosidade de fundo e viscosidade horizontal sendo posteriormente validado. Os dados usados para esta componente do trabalho foram recolhidos por investigadores do CIMA no âmbito de projetos de investigação (e.g. Jacob et al., 2013). O objetivo neste processo é ter um modelo de linha de base confiável para avaliar alterações de longo prazo induzidas pela SNM na circulação das marés. 4 cenários diferentes de SNM no ano 2100 (SLR = 0.47 m, Antunes e Taborda, 2009; SLR = 0.53 m, IPCC, 2014; SLR = 0.74 m, IPCC, 2014; SLR = 0.84 m, Jackson and Jevrejeva, 2016) foram considerados para avaliar os impactos de SNM na hidrodinâmica da lagoa. Vários pontos de observação e seções transversais do modelo foram usados para estudar as variações locais nos impactos SLR na assimetria prevista das marés, velocidades médias da corrente e velocidades máximas da corrente dentro da lagoa.

Alguns parâmetros do modelo de malha estruturada foram ajustados a partir do modelo calibrado e validado usado por González-Gorbeña et al. (2018) para melhor se adequar ao presente foco de investigação. A área de estudo foi ampliada para o Canal do Ramalhete e seus arredores para estudar a evolução morfológica de longo prazo sob SNM dentro da lagoa. Testes de sensibilidade foram realizados para selecionar valores apropriados de fator de aceleração morfológica (Morfac), coeficiente de rugosidade do fundo e tamanho médio de grão do

sedimento (D50) para o presente estudo. Os valores selecionados de Morfac (100), D50 (175 µm) e coeficiente de Manning de rugosidade do fundo (variando de 0,05 m2/s no mar a 0,4 m2/s nos sapais) encurtam consideravelmente os tempos de simulação e foram considerados mais adequados para representar os efeitos de longo prazo da SNM na evolução morfológica dentro da lagoa. O tempo total de simulação (89 anos) foi dividido em três simulações de 25 anos e uma simulação final de 14 anos. A batimetria inicial foi atualizada entre as simulações, utilizando a batimetria do final do período de simulação anterior para o início da simulação. O modelo foi forçado por: (a) maré M2; (b) uma correção de amplitude para M2 e (c) uma maré esquematizada com base na assimetria de maré entre as componentes de maré O1 e K1 e a componente M2.. Uma taxa de SNM linear de 1,1 mm/ano, que deriva de um valor de SNM de 0,98 m no ano 2100, foi forçada no modelo. Diferenças de elevação para os cenários de linha de base (sem SNM) e de SNM, para o ano 2100 e para cada intervalo de simulação, foram representadas para o setor oeste da Ria Formosa e para o Canal do Ramalhete e arredores. Os pontos de observação e seções transversais foram modelados em aproximadamente os mesmos locais para aqueles usados no modelo de malha não estruturada para estudar as variações locais nos impactos da SNM. O objetivo de usar localizações aproximadas foi tentar de manter a consistência entre os resultados de ambas abordagens de modelação, e investigar se mudanças batimétricas ocorrem nas áreas onde são esperados impactos na hidrodinâmica da lagoa induzidos pela SNM. Diferenças no deslocamento do canal e perfis transversais de profundidade para ambos cenários, no ano 2100 e para cada intervalo de simulação, foram calculadas ao longo de cada uma das seções transversais modeladas. As taxas máximas de alterações transversais na batimetria foram calculadas para cada seção transversal e discutidas para ambos cenários.

Os resultados do modelo de malha não estruturada destacam o impacto da SNM na distorção das marés da lagoa, uma vez que a dominância da enchente na Barra do Ancão aumenta proporcionalmente à intensidade da SNM. A SNM também perturba as velocidades máximas da corrente e em algumas partes do Canal de Faro existe uma alteração no período em que a velocidade da corrente atinge o seu valor máximo. Os resultados obtidos implicam um aumento do papel da Barra do Ancão na hidrodinâmica da Ria Formosa e apontam para futuras perturbações do transporte residual de sedimentos, que se espera induzirão alterações batimétricas. Em contraste, os impactos da SNM na morfologia da lagoa são geralmente pequenos. As alterações batimétricas no Canal do Ramalhete e seus arredores aparecem relativamente pequenas, com valores de erosão no ano 2100 inferiores a 0,1 m e nenhum deslocamento do canal visto, mesmo nos intervalos de simulação posteriores. Em geral, nos

sapais a erosão prevalece sobre a acumulação e a intensidade da erosão aumenta ligeiramente para cerca de 0,3 m. A falta de diferenças de elevação maiores sugere que os sapais serão capazes de se ajustar à SNM, mas também deve ser considerado que em condições de baixo transporte de sedimentos, a capacidade de sobrevivência dos sapais à SNM é bastante reduzida. Não são previstos grandes impactos na economia ou na ecologia da lagoa. Algumas limitações foram encontradas na modelação das interações do sedimento e a implementação da tendência da SNM e a não inclusão de um modelo de ondas reduz a confiabilidade do modelo.

Em resumo, podemos concluir que a SNM alterará a distorção das marés e os padrões de transporte residual de sedimento dentro da lagoa da Ria Formosa, e que mais estudos são ainda necessários para abordar, de forma confiável, as mudanças morfológicas de longo prazo induzidas pela SNM na lagoa. Este estudo contribui para o conhecimento científico sobre os impactos da SNM nas lagoas costeiras e fornece uma primeira abordagem para analisar a evolução morfológica de longo prazo da SLR na lagoa da Ria Formosa.

# Chapter 1 - Introduction

## 1.1. Motivation for the topic

Sea level rise (SLR) is one of the most studied physical consequences of climate change in the scientific community, as 10% of the population live within 10 m of elevation from present sea level (Carrasco et al., 2016). Increased coastal flooding, altered inundation patterns, saltwater intrusions into fresh waters, loss of coastal wetlands and changes in local hydrodynamics are the most important impacts caused by SLR (Bilskie et al., 2014). Lately, instead of the global-mean projected SLR rate, many authors have identified Relative Sea Level Rise (RSLR) as a critical variable for local SLR impacts (e.g., Church and White, 2006; Kirwan and Murray, 2008; Gillanders et al., 2011). Among the more important coastal areas affected by RSLR are coastal lagoons, as they are highly productive areas and cover ~13% of the global coastline (Kjerfve, 1994; Carter and Woodroffe, 1994). Carrasco et al. (2016) stressed in a recent review that perhaps the most serious and widely recognized issue facing coastal conservation is the impact of RSLR on coastal landforms in coastal lagoons and estuaries. Most coastal lagoons are maintained only by the protection afforded by barriers and spits, presenting very peculiar feedbacks to RSLR (List et al., 1997). The impact of RSLR in coastal lagoons might cause the loss of key ecological components such as salt marshes, or even the complete disappearance of the lagoon (Van Goor, 2003; Bilskie et al., 2014).

Despite the existence of several studies exploring the effect of SLR globally and in Portuguese coasts (e.g. Nicholls, 2004; Lopes et al., 2011; Mendes et al., 2013) the impact of SLR in the Ria Formosa coastal lagoon is still largely unexplored. Recently, Carrasco et al. (2018) provided the first study to research the effects of SLR in the hydrodynamics of the Ria Formosa lagoon and stressed the need for further research focusing on the quantification of the physical and socio-economic impacts of SLR on lagoon systems. This master thesis investigates the long-term impacts of different scenarios of SLR on the local tide circulation and morphological evolution of the Ria Formosa lagoon. This study aims to contribute with modelling results to the research gap in the effects of SLR in coastal lagoons, to improve the existing knowledge about the coastal dynamics of the Ria Formosa lagoon and to contribute to the overall knowledge about coastal lagoons resilience facing sea-level rise scenarios.

## 1.2. Main objectives of the study

The main objective of this project is to investigate the long-term (c. 100 years) impact of different SLR scenarios in the tide circulation and channel morphodynamics in the Ria Formosa lagoon using numerical modelling. Other goals are to contribute to the overall understanding about how SLR is likely to affect coastal lagoons, in terms of tidal asymmetry and tidal prisms inside the lagoon, current velocities, sediment erosion and deposition throughout the lagoon, morphological evolution of channels and salt marsh deposition.

# Chapter 2 - State of the art

## 2.1. Coastal lagoon characteristics

Coastal lagoons can be defined as "shallow water bodies, separated from the ocean by a barrier, connected at least intermittently to the ocean by one or more restricted inlets" (Kjervfe, 1994) and their existence is dependent on the stability of the barrier enclosing them (Nicholls and Boon, 1994). Sea-level history, shoreface dynamics and tidal range are the three main factors that determine the stability of sandy barriers (Martin and Dominguez, 1994; Anthony, 2009). Sea-level rise has the potential of disrupting tidal hydrodynamics by increasing tidal range, volume of tidal prisms (total volume of water leaving the estuary during the ebb period) and inundation (Carrasco et al., 2018). In coastal lagoon environments, tide wave propagation through the shallow channels is the main factor controlling sedimentation and the local ecology (Aubrey and Speer 1985; Friedrichs et al. 1990; Van Goor et al. 2003). The discrepancies in tide wave propagation within the lagoon induce tidal asymmetry (difference between maximum intensity and duration of the flood and ebb periods of an estuarine system) and establish sediment circulation patterns within the channel (Dronkers, 1986; Carrasco, 2018). Tidal asymmetry can be assessed in terms of strength (i.e. imbalance between the contributions of the different harmonic tide constituents) and type (flood-dominant or ebb-dominant, depending on which period has a higher duration). Coastal lagoons and estuaries with tidal flats often are ebb-dominant, which can cause seaward residual transport (Stark, 2017). SLR increases channel depth or changes the volume of water stored in the intertidal zone, fundamentally altering tidal asymmetry and sediment transport patterns (Carrasco et al, 2018). SLR also has the potential to alter lagoon flushing rates (i.e. the rates at which water enters, circulates through, and exits from lagoons; Anthony et al., 2009; Carrasco et al., 2018)

and modify current velocity distribution (which is known to be sensitive to the effect of tidal asymmetry in average and peak tidal ebb/flood velocities; Jewell et al., 2012).

## 2.2. Morphological response to SLR

A tidal system with its dynamic equilibrium distorted by RSLR tends to accumulate sediment as a mean to restore it, with the amount of sediment required for this restoration being proportional to the RSLR (Louters and Gerrisen, 1994). When accumulation rate is higher than the RSLR rate the response of the system to RSLR is delayed, and when the RSLR rate is consistently higher for enough time the system loses its dynamic equilibrium (Louters and Gerrisen, 1994); these evolution patterns were confirmed in Venice Lagoon by Defina et al. (2007). Sediment accumulation can cause bathymetric changes, such as the ones reported by Lopes et al. (2011) in the Ria de Aveiro, due to an intensification in sediment fluxes and an increase of 28% of the tidal prism at the lagoon mouth. As morphologies in coastal lagoons cover from a cm-m scale in the case of bedforms to ~1-100 km in the case of the full basin (Carter and Woodroofe, 1994; Hibma et al., 2004), the response of the lagoon to SLR varies within the lagoon.

RSLR can cause either an import or an export of sediment to the channels, depending on local conditions such as tidal velocity or local basin geometry (Friedrichs et al., 1990). In addition, the relationship between changes in tidal prism and tidal channels width and depth was reported in the recent review by Coco et al. (2013) and in the similar findings by Stefanon et al. (2012); they stated that a decrease on the tidal prism leads to smaller channel cross-sections and a general retreat of the channels, and that the opposite effect occurs with an increase in tidal prism (Stefanon et al., 2012). The sediment deposition rates in salt marshes are a good way of assessing the maturity of coastal lagoons and assessing the marsh ecological ability to cope with SLR (e.g., Edwards, 2007; Cronin, 2012). Salt marshes are important components of coastal lagoon ecosystems and there is the possibility of them being negatively affected by SLR, forcing them to migrate or even disappear (Bilskie et al., 2014). Rizzetto and Tosi (2012) found that in the Venice Lagoon, rising water levels and the frequency of high tides greatly influenced shifts in the margins of the salt marsh and meander evolution in the long-term, that will lead to tidal channel development in the current salt marsh habitats.

Barrier islands tend to progressively migrate inland with SLR (e.g. Zhang et al., 2004; Masetti et al., 2008; Moore et al., 2010), although the migration rate can be affected by other factors such as stratigraphy (e.g., Storms et al., 2002; Moore et al., 2010) or sediment grain size

(e.g., Storms et al., 2002; Masetti et al., 2008) and can respond in a myriad of ways (Figure 2.1). Some authors, such as Van Goor et al. (2003), determined that in a context of constant SLR, a tidal inlet system would permanently lose its equilibrium state, leading to a change in its dynamic state or even to its disappearance. Fitzgerald et al. (1984) reported that changes in hypsometry in the Friesian Islands led to a reduction of the tidal prism and the narrowing of the inlets by 52%. However, these findings are not consistent with the ones of Fitzgerald et al. (2006), who reported in a study performed in worldwide embayments (e.g. East Coast of the United States, North Sea, Gulf of Alaska) that changes in the hypsometry of the basin might convert backbarrier systems to open water, increasing the tidal prism, reducing the area of barrier islands and widening the inlets. These later findings were confirmed for the Amenland Inlet in the study case of Dissanayake et al. (2012).

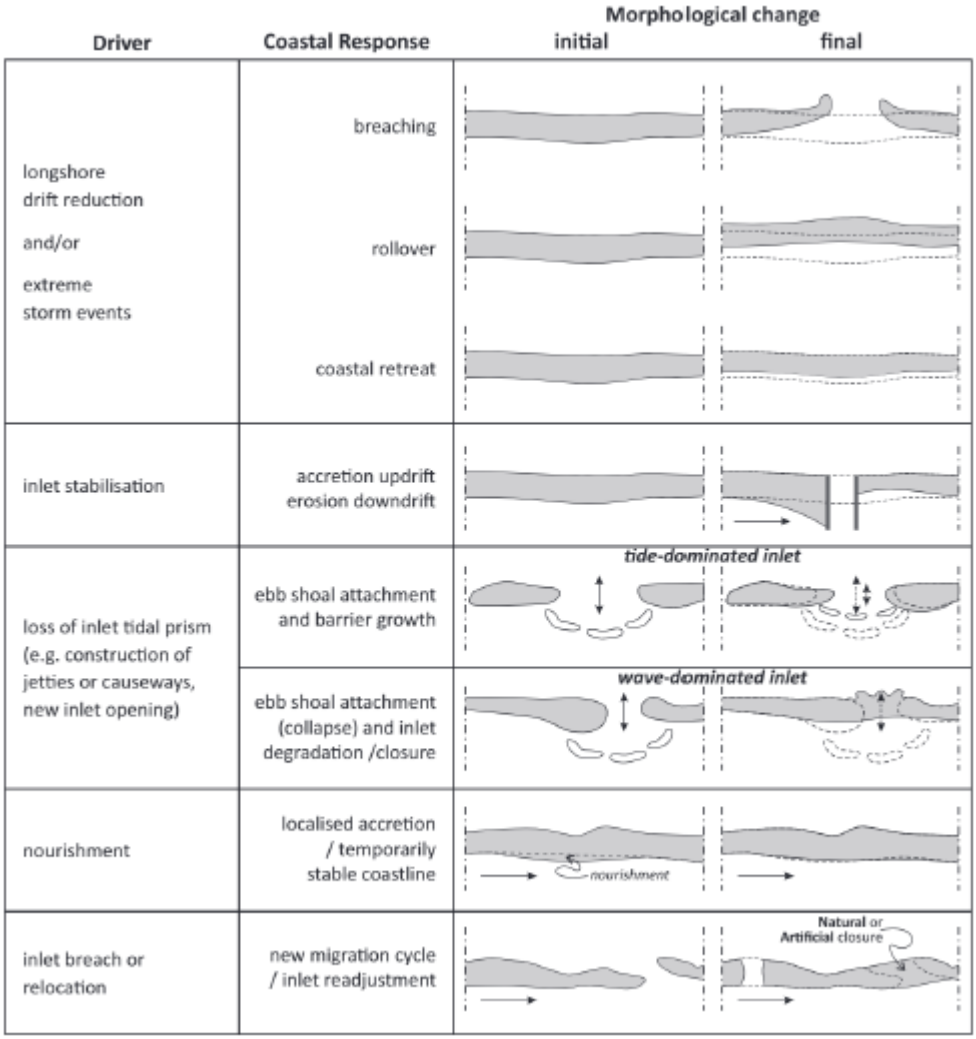


Figure 2.1. Schematic representation of main artificial triggers (AT) and natural drivers (ND) of barrier morphological change and induced changes. Figure source: Kombiadou et al. (2019).

The previously mentioned studies contribute to the knowledge about SLR impacts in the morphological evolution of coastal lagoons; however, Carrasco et al. (2016) stressed the need for further research in all scales (especially small scales, such as tidal channels or tidal inlets). Therefore, future studies should improve the knowledge on the morphological threshold above which bathymetry features are eroded, and focus on local individual lagoon systems and their potential evolutions in response to SLR up to a century, among others (Carrasco et al., 2016). Finally, Walters et al. (2014) addressed that little is known about how the connectivity of the two constituent landscape systems (i.e., barriers and inlets) affects the evolution of coupled barrier–marsh systems under changing conditions; therefore, more studies about that connectivity, as well as studies exploring the effect of SLR over it, should be explored in the future.

## 2.3. Modelling of SLR impacts

Numerical models relating SLR and coastal evolution have significantly evolved over the last 20 years and currently are a major tool for gaining insights into tidal asymmetry, impacts induced by SLR, backbarrier stability and resilience (Roelvink, 2006; Carrasco et al., 2016). Models can be divided into three main groups: simple shoreline models, behavior models, and process-based models. Especially, recent process-based circulation models such as Delft3D (e.g. Lesser et al., 2004; González-Gorbeña et al., 2018) have demonstrated success at modelling hydrodynamics and morphology from short- (i.e. local inundation events) to long-term (i.e. effects of sea-level rise) scales when coupled with sediment transport processes (Lesser et al., 2004; Roelvink, 2006; Carrasco et al., 2016). Many studies have explored future SLR effects using several projected scenarios (alternative images of the future) of Global Mean Sea Level based on current SLR rates, which has facilitated assessing the impacts of SLR in too complex and/or uncertain systems (e.g. Nicholls et al., 2014; Jackson and Jevrejeva, 2016). Lately, instead of the global-mean projected SLR rate, many authors have identified Relative Sea Level Rise (RSLR) as a critical variable for local SLR impacts (e.g., Church and White, 2006; Kirwan and Murray, 2008; Gillanders et al., 2011). Local processes such as subsidence, thermal expansion and isostatic adjustment have been recently proposed as causes for RSLR (Slangen et al., 2012; Jackson and Jevrereva, 2016).

The latest modelling studies performed in the Ria Formosa are those of Carrasco et al. (2018) and Gonzalez-Gorbeña et al. (2018), who applied models built in the Delft3D domain for different purposes. Carrasco et al. (2018) used a process-based model solved in an

unstructured mesh to evaluate the patterns and effects of Relative Sea Level Rise on the tidal circulation of the basin of the Ria Formosa coastal lagoon, while Gonzalez-Gorbeña et al. (2018) used a structural modelling grid approach to estimate the optimum size of a tidal array. These two modelling approaches were the ones followed in this study to predict the effect of SLR in the hydrodynamics and morphodynamics of the Ria Formosa.

# Chapter 3 - Study Area: Ria Formosa coastal lagoon

## 3.1. Location and characteristics

The Ria Formosa is a barrier island system located in Southern Portugal with five islands and two peninsulas, separated by six tidal inlets: Ancão Inlet, Faro-Olhão Inlet, Armona Inlet, Fuzeta Inlet, Tavira Inlet and Lacém Inlet (Fig. 2). The lagoon can be divided in three water sub-embayments, with the Ancão, Faro-Olhão and Armona inlets comprising the western sector; the Fuzeta and Tavira inlets comprising the central sector; and the Lacém Inlet comprising the eastern sector (Salles et al., 2005).

The lagoon has a triangular shape and is about 55 km long (E-W) and 6 km wide (N-S) at its widest zone (Figure 3.1). It has about 105 $km^2$ of wet area, including a large intertidal zone. The embayment is composed of large salt marshes, sand flats and a complex net of natural and partially dredged tidal channels. The salt marshes comprise silt and fine sand (Bettencourt, 1994) and are intersected by a high density of shallow meandering tidal creeks. The Ria Formosa is a Natural Park, holds target habitats for conservation (EU Habitat Directive) and is protected by the Natura 2000 network. Beyond the tourist use (mostly ecotourism and leisure holidays), the system also supports other economic activities, like several seafood farms scattered through the lagoon (Ministério do Ambiente e Ação Climática, 2017) and the use of the port of Faro.

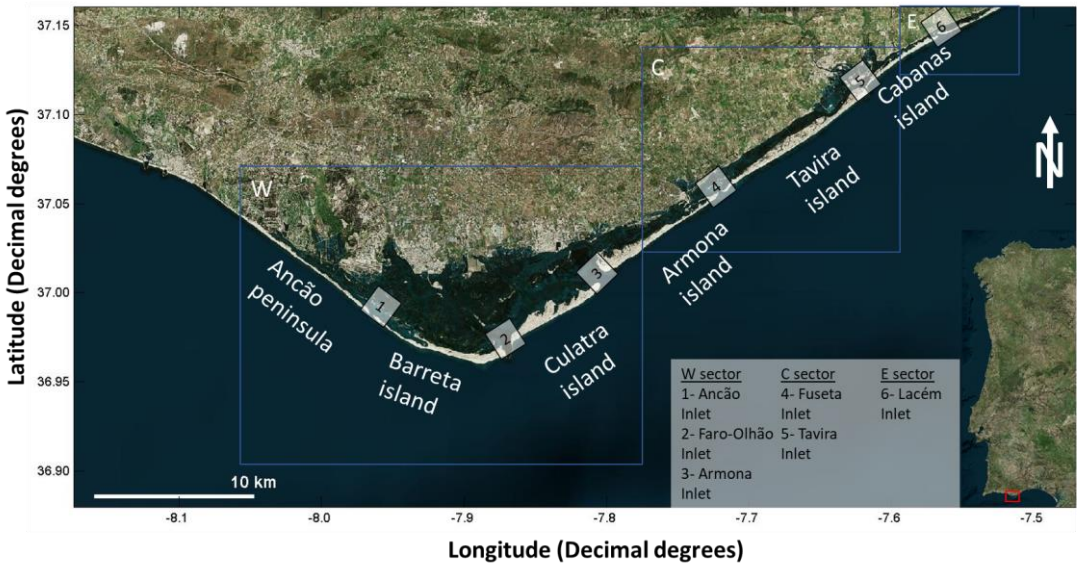


Figure 3.1. Study area, the Ria Formosa Lagoon (South of Portugal). (Jan 2018, from Bing Maps).

## 3.2. Hydrodynamic conditions in the lagoon

The tidal inlets behavior, mostly from the western sector of the Ria Formosa, presented in the past a significant contribution to the evolution of barriers and channels (Vila-Concejo et al., 2004). The tides in the area are semi-diurnal, with typical average ranges of 2.8 m for spring tides and 1.3 m for neap tides, and a maximum tidal range of 3.5 m in equinoctial tides. The offshore annual mean wave height (Hs) is ~1m with a peak period (Tp) of 8.2 s, with ~71% of the waves approaching from the W-SW and ~23% approaching from the E-SE (Costa et al., 2001). Estimates for the minimum submerged area of the Ria Formosa are 53 $km^2$ at high-water and 14-22 $km^2$ at low water (Dias et al., 2009)

Pacheco et al. (2010) found that ~90% of the total tidal prism in the Ria Formosa system is captured in the western sector: the Faro-Olhão Inlet (the main stabilized one) has a residual prism oriented landward of ~61% of the total tidal prism in the lagoon in spring tide and of 45% in neap tide; the Armona Inlet (the historically more persistent one) has a residual prism oriented offshore of ~23% in spring tide and of 40% in neap tide; and the Ancão inlet has a residual prism of ~8%, oriented offshore, in spring tide, and of lower importance, oriented landward, in neap tide. These inlets have a strong interconnection degree, and their evolution does not seem to be approachable deriving from inlet hydraulics or using empirical equilibrium relations (Pacheco et al., 2010). The two main inlets (Faro-Olhão and Armona) are always interconnected, transferring large portions of the tidal prism between them, and draining the basin more independently for a portion of the neap-spring tidal cycle (Pacheco et al., 2010). Pacheco et al. (2010) also found that although residual flow and the morphology of the inner

channels can play an important role in enhancing stability, they are not sufficient to counteract the entry of sediment under wave-current interactions and during periods of storm activity. These findings agree with the hypothesis proposed by other authors (Salles et al., 2005) that the capacity to exchange large portions of prism independently of the tidal cycle, can contribute to the stability of multiple inlets.

### 3.3. Morphological evolution of the Ria Formosa lagoon

The evolution of the Ria Formosa lagoon is intrinsically linked to human interventions. The opening of the artificial inlets of Tavira (opened in 1927) and Faro-Olhão (opened in 1929) fundamentally changed the hydrodynamic circulation of the lagoon; after the stabilization of these new inlets, the tidal prism of the Armona Inlet (the main inlet of the lagoon until the opening) was significantly reduced and Faro-Olhão became the main inlet of the lagoon (Pacheco, 2010). Other hard engineering works performed over time include construction of a 600 m rubble mound revetment in west Culatra (between 1958 and 1972), construction of jetties in Vilamoura (1972), construction of a 1200 m seawall in the central part of the Ancão Peninsula (mid-1980s) and stabilization with jetties and conversion to rubble mound of a 750 m stretch along the west lagoon-side coastline of Culatra (late 1980s) (Kombiadou et al., 2019). Finally, the Ancão and Fuzeta inlets have been relocated on several occasions (the first time in 1997 and 1999, respectively; Vila-Concejo et al., 2004) to improve water quality and circulation of the lagoon and to recover the dynamic equilibrium of the system. While the relocation of the Ancão Inlet was considered successful, the Fuzeta Inlet had the same problems that it had before being relocated, proving that the hydrodynamics of the Ria Formosa are challenging to study and that more hydrodynamic studies were needed (Vila-Concejo et al., 2004). Overall, human interventions have defined the hydrodynamic and morphological evolution of the Ria Formosa lagoon; the findings of Kombiadou et al. (2019) estimated that human interventions in the lagoon had a decisive influence in the increase of barrier island coverage by 15%.

Although several studies about hydrodynamics and morphological evolution in the Ria Formosa lagoon have been done recently (Duarte et al., 2008; Pacheco et al., 2008; Dias and Sousa, 2009; Cravo et al., 2013; Kombiadou et al., 2019; Jacob et al., 2019; Rosa et al., 2019), only one study has researched SLR impacts in the hydrodynamics of Ria Formosa (Carrasco et al., 2018) and no studies have been done exploring the morphological evolution of the Ria Formosa lagoon under SLR. This study aims to be one of the first to explore those topics and provide reliable data about the hydrodynamic of the Ria Formosa western sector under SLR

scenarios; the modelled data is expected to be useful for ecosystem evolution studies and long-term coastal management.

# Chapter 4 - Methodology

To explore the effects of SLR in the channels (Faro, Ramalhete and Ancão) and inlets (Faro-Olhão, Armona and Ancão) of the western sector of the Ria Formosa, the long-term hydrodynamic and morphodynamic processes under current conditions and under hydrodynamic conditions forced by SLR were simulated. In this study two models built in the Delft3D domain were used: one with an unstructured grid modelling approach and one with a structured grid modelling approach. During model setup, an unstructured grid modelling approach was favoured to simulate long-term changes in hydrodynamic and morphodynamic processes, but computational mistakes kept hindering the simulation of morphodynamic processes. Consequently, long-term changes in morphodynamics processes (as well as the governing hydrodynamic processes they are dependent on) were simulated with a structured grid modelling approach. To study the effects of SLR in the morphological evolution of the tidal channels, the study area was zoomed to the Ramalhete Channel. This tidal channel presents commercial value, associated to its exploitation as a local waterway and the presence of oyster farming areas in the channel margins, and ecological value, associated to the presence of salt marshes along the full length of the channel.

## 4.1. Unstructured grid model

### 4.1.1 Basic setup

This study applies a 2DH (two-dimensional) modelling approach previously used by Carrasco et al. (2018) comprising five stages: generation of the model grid, generation of boundary forcing, model calibration, model validation, and running scenarios. The numerical model applied in this work is the Delft3D Flexible Mesh, a process-based unstructured grid finite volume model developed by Deltares (Kernkamp et al., 2010; Deltares, 2016). The domain for our study extends from Armona Inlet up to the western limit of Ancão Peninsula, reaches approximately 2 km offshore and exceeds 30 km in the alongshore direction (western part of Ria Formosa lagoon, Figure 4.1). The average cell size ranges from 50 x 50 m at inlets to 20 x 10 m at the inner channels. Local elevation (bathymetry and hypsometry) was obtained from LIDAR data from 2011.

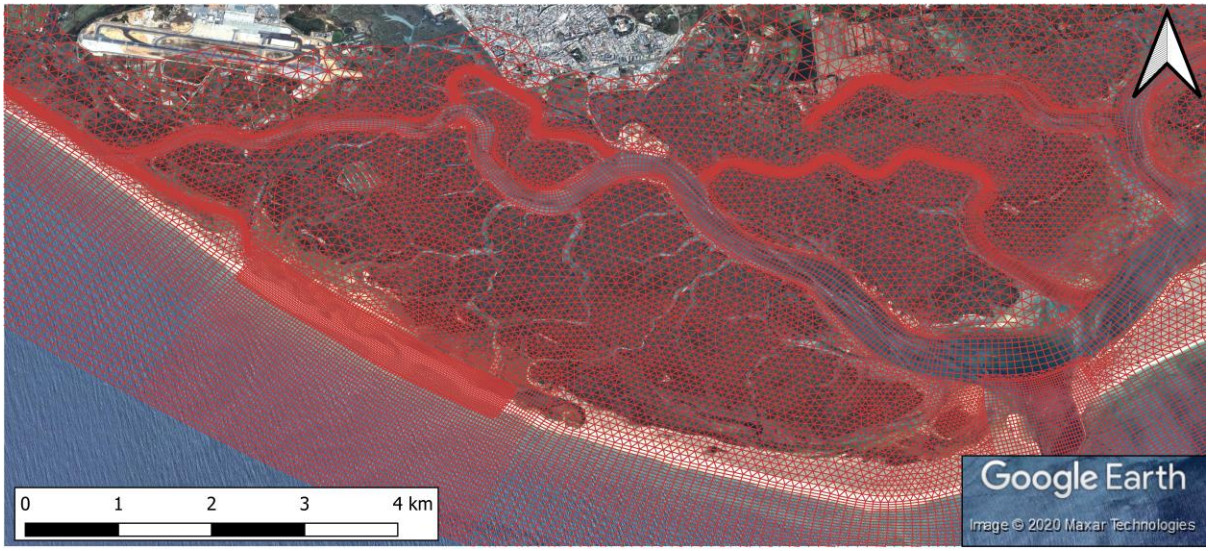


Figure 4.1. Grid used in the present modelling approach to simulate hydrodynamics in the Ria Formosa lagoon. A darker red colour indicates a higher grid density and therefore a higher resolution. (Source: "Western Ria Formosa". 36.980414º N and 7.884412º W. Google Earth. December 31st, 2011. Retrieved September 25th, 2020)

The model was forced with an offshore water level boundary and two lateral water level gradient boundary conditions (Neumann boundaries) with the local main tidal constituents (M2, S2, N2, K2, K1, O1, P1, Q1, MF, MM, M4, MS4, MN4); the offshore boundary is close to the lagoon and tidal wave energy absorbed by the lagoon system. Amplitudes and phases of the constituents were derived from the TPXO global tidal model (Egbert and Foremann, 1994).

### 4.1.2. Assessment of the unstructured model performance

The model performance of the calibrated (and validated) model was assessed in terms of three main error parameters: (1) the bias, (2) the root mean-square error (RMSE) and (3) the skill parameter, as seen in Carrasco et al. (2018). The bias measures the difference between values predicted by the model ($x_{modelled}$) and values observed in the field ($x_{measured}$) and is determined by:

$$bias(x) = \frac{1}{N}\sum_{i=1}^{N}(x_{i,modelled} - x_{i,measured}) \quad (1)$$

where $x_{modelled}$ is the observed value and $x_{measured}$ is the modelled value. The RMSE is the square root of the mean squared error, determined by:

$$RMSE\ (x) = \sqrt{\frac{1}{N}\sum_{i=1}^{N}(x_{i,modelled} - x_{i,measured})^2} \quad (2)$$

The RMSE indicates the variability between model results (from calibration and validation) and data (e.g. water level time series), being zero when the model and data present

the same value.

The skill measure (from Dias et al., 2009) is used to evaluate all prognostic quantities, and determines agreement between model results and observations:

$$Skill = 1 - \frac{\sum(x_{i,modelled} - x_{i,measured})^2}{\sum(|x_{i,modelled} - \overline{x_{i,measured}}| + |x_{i,measured} - \overline{x_{i,measured}}|)} \quad (3)$$

Perfect agreement between model results (from calibration and validation) and observations yields a skill of one, and complete disagreement yields a skill of zero. Skill values higher than 0.95 are considered representative of an excellent agreement between model results and observations. Bias, RMSE and the predictive skill were applied to the observed and simulated time series (water levels and depth-averaged currents).

### 4.1.3. Spin-up time adjustment in the unstructured model

The spin-up time adjustment was done before the model calibration (and validation) and consisted in determining the required number of cycles (time) so that the model can adjust to the external forcing, and its results are considered as representative of the real conditions. To ensure the optimal starting data, 5 spin-up times were tested: 21, 16, 11, 8, and 5 days of simulation. The model results were compared with a dataset with measurements taken over 30 days, from the Cais Comercial station of the COALA project (Table 4.1). For spin-up assessment, the model was set up with a Manning coefficient of 0.020 $m^2/s$ and a horizontal eddy viscosity of 1 $m^2/s$ (Table 4.2). Initial water conditions derivate from the historic MSL records from the closest tide gauge available, the Huelva tide gauge (Ministerio de Transportes, Movilidad y Agenda Urbana, 2020).

Table 4.1. Datasets used for the spin-up time, model calibration and model validation.

| ***Data for calibration*** | ***Year*** | ***Associated Project*** | ***Data type*** | ***Length of datasets*** | ***Location in the model (etrs89 utm29) x/y*** |
|---|---|---|---|---|---|
| Cais_comercial | 2012 | COALA | water level; pressure transducer | 30 days | 596291.1875/4095693.25 |
| Deserta | 2012 | COALA | water level; pressure transducer | 30 days | 600540.5/4091709.75 |
| Praia_Faro bridge | 2013; 2014 | - | water level; pressure transducer | 7 days | 589542.625/4096356.75 |
| Bar da Gina | 2012 | Maré Formosa | water level; ADP measurements | 1 day | 589197.9375/4096615.5 |
| Centro Naútico | 2012 | Maré Formosa | water level; ADP measurements | 1 day | 590227.9197/4095692 |
| Canal Cações | 2012 | Maré Formosa | water level; ADP measurements | 1 day | 601380.25/4096465.75 |
| Marim | 2012 | Maré Formosa | water level; ADP measurements | 1 day | 605728.3125/4098435.25 |
| Armona Inlet | 2012 | Maré Formosa | water level; ADP measurements | 1 day | 606314.4375/4096452.25 |
| ***Data for model validation*** | ***Year*** | | ***Data type*** | | ***Location in the model x1/y1 x2/y2*** |
| FO Inlet | 2006 | CIMA data | Averaged velocities; ADCP measurements during spring and neap tides | 1 day | 600751.000000/4092466.250000 600124.312500/4092173.250000 |
| Armona Inlet | 2007 | CIMA data | Averaged velocities; ADCP measurements during spring and neap tides | 1 day | 606448.875000/4096930.250000 606523.875000/4096414.000000 |

Table 4.2. Generic model configuration.

| Model setup parameters | Values |
|---|---|
| ***Numerics:*** | |
| Courant number | 0.7 |
| Gravitational acceleration | 9.81 $m/s^2$ |
| Water density | 1025 $kg/m^3$ |
| ***Physics:*** | |
| Uniform friction coefficient | 0.02 $m^2/s$ |
| Friction formulation | Manning |
| Uniform horizontal eddy viscosity | 1$m^2/s$ |
| Uniform horizontal eddy diffusivity | 1$m^2/s$ |
| ***Time:*** | |
| Time step | 60 sec |
| Maximum Time step | 60 sec |
| Time units in MDU file | minutes |
| ***Output format:*** | |
| Observational point interval | 600 sec |
| Map interval | 3600 sec |

The bias, RMSE and Skill parameters showed little difference between using a spin-up time from 21 to 8 days, but the values showed a worst agreement for a spin-up time of 5 days; therefore, a spin-up time of 8 days was selected for all the simulations.

### 4.1.4 Unstructured model calibration

The unstructured model was calibrated by adjusting the bottom roughness local value and the horizontal eddy viscosity for the Ria Formosa present conditions. Two different Chézy coefficients (60, 65 $m^{1/2}/s$), three different Manning coefficients (0.018, 0.020, 0.023 $m^2/s$), and a depth-integrated Manning coefficient approach were used for tuning the most reasonable bed roughness variability. The horizontal eddy viscosity was tuned by applying two viscosity constants, 1 and 0.5 $m^2/s$. The bottom roughness runs were set up with a horizontal eddy viscosity of 1 $m^2/s$, while the horizontal eddy viscosity runs were set up with a Manning's coefficient of 0.020.

The calibrated model performance was assessed by comparing the calibrated model results with local measurements (water-levels) from eight different stations scattered around the Ria Formosa (Table 4.1, Figure 4.2), using the aforementioned bias, RMSE and skill parameters. Measurement stations are mostly distributed along the main lagoon channel, Faro Channel, and contain hourly water-level data series (e.g. Jacob et al., 2013).

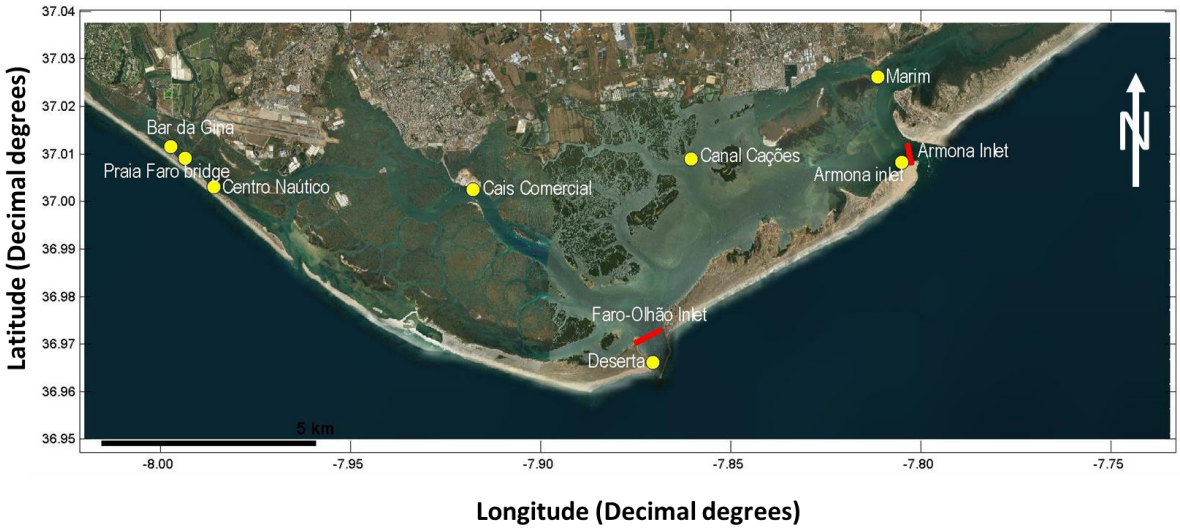


Figure 4.2. Location of the eight measurement stations (yellow circles) scattered around the Ria Formosa; red lines represent cross-shore depth averaged velocity measurements used in the validation process.
(Jan 2018, from Bing Maps).

The model calibration results showed that some stations, such as Bar da Gina and Marim, presented higher values of bias and RMSE for most model setups than other stations (Figure 4.3), and they also showed lower skill values (Figure 4.4). Nevertheless, most stations showed a skill value of 0.95 or higher, which indicates an excellent agreement. When examining the accumulated error results, the model setup "Viscosity" (Manning's coefficient of 0.020 $m^2/s$, horizontal eddy viscosity of 0.5 $m^2/s$) was the one carrying lowest accumulated RMSE (Figure 4.5). This latter was the setup selected as the final calibrated model.

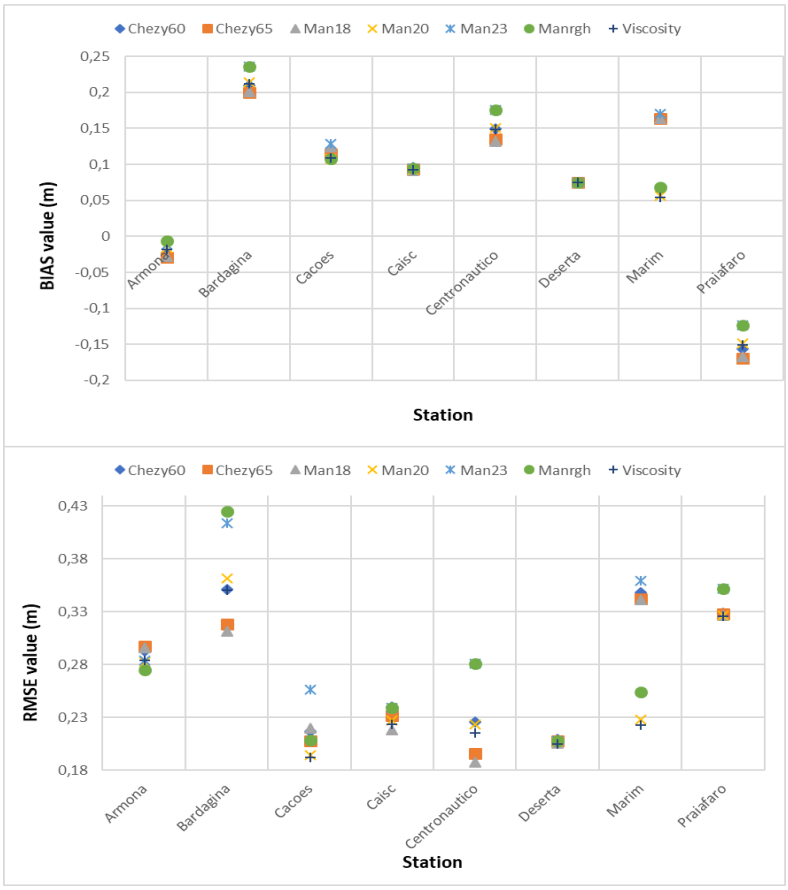


Figure 4.3. Distribution by station of Bias values (upper graph) and RMSE values (lower graph) of water elevation for the full datasets (see Table 1).

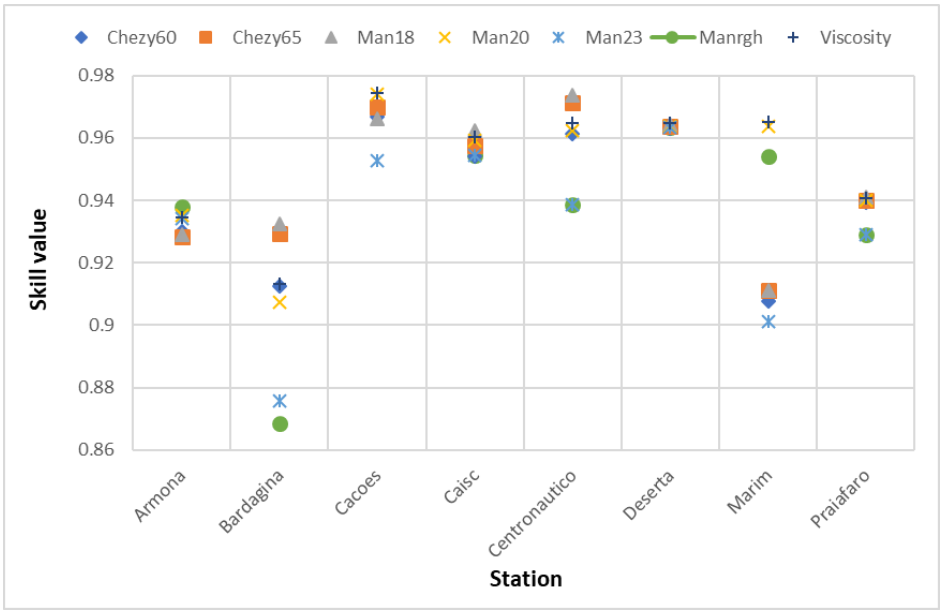


Figure 4.4. Skill distribution by stations.

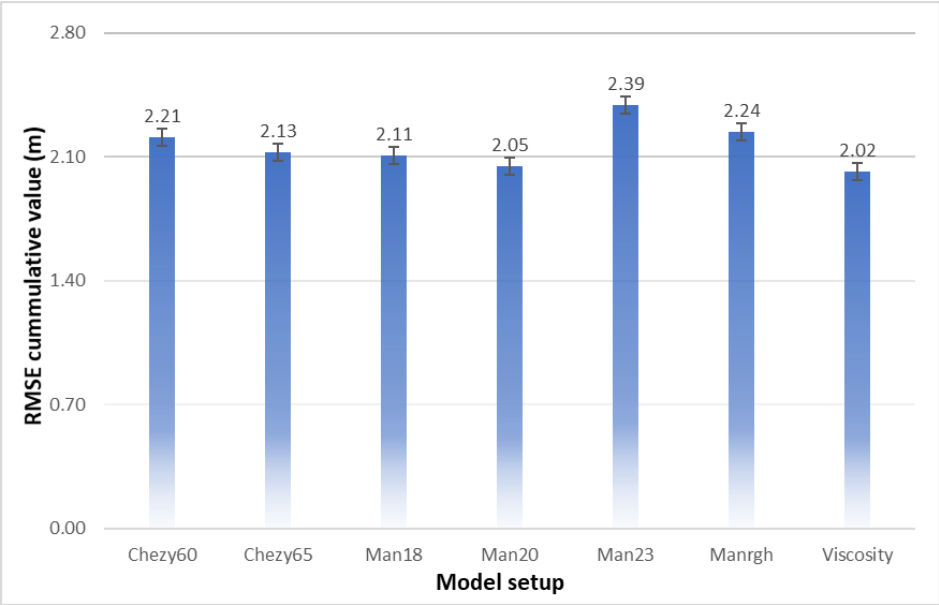


Figure 4.5. Sum of the individual RMSE of all stations for each model setup.

### 4.1.5 Unstructured model validation

After the calibration process, the selected setup for the model must be validated using independent measurements, to better assess the model's suitability for the area. During model validation, depth-averaged velocities obtained in the calibrated model were compared with depth-averaged current velocities datasets, measured by CIMA researchers across the sections of Faro-Olhão and Armona inlets. Two tide conditions were compared: spring tide and neap tide (Table 4.1, Figure 4.6), and the skill parameters (defined in section 4.1.2) were again used to assess the performance of the validated model.

The results of the validation process showed a good agreement between the modelled after calibration (predictions) and observed results (measurements), with three out of four of the currents data showing an excellent agreement (skill over 0.95, Table 4.3) with the calibrated model setup. The performance results of the Armona Inlet data show a better agreement between predictions and measurements than the Faro-Olhão Inlet data, for both spring tides and neap tides (Figure 4.6). The model slightly underestimates the velocity of the currents in the Faro-Olhão Inlet in neap tide, with velocities in a range of -0.1 to 0.1 m/s compared to the recorded range of -0.25 to 0.25 m/s. Nonetheless, the high skill and low RMSE values indicate a good overall representation of the hydrodynamic processes of the Ria Formosa.

Table 4.3. Bias, RMSE and skill values for the currents data.

| Inlet | Tidal range | Bias (m/s) | RMSE (m/s) | Skill |
|---|---|---|---|---|
| Armona | Neap tide | -0.04 | 0.11 | 0.96 |
| Armona | Spring tide | 0.08 | 0.15 | 0.96 |
| Faro-Olhão | Neap tide | 0.03 | 0.17 | 0.86 |
| Faro-Olhão | Spring tide | 0.03 | 0.15 | 0.96 |

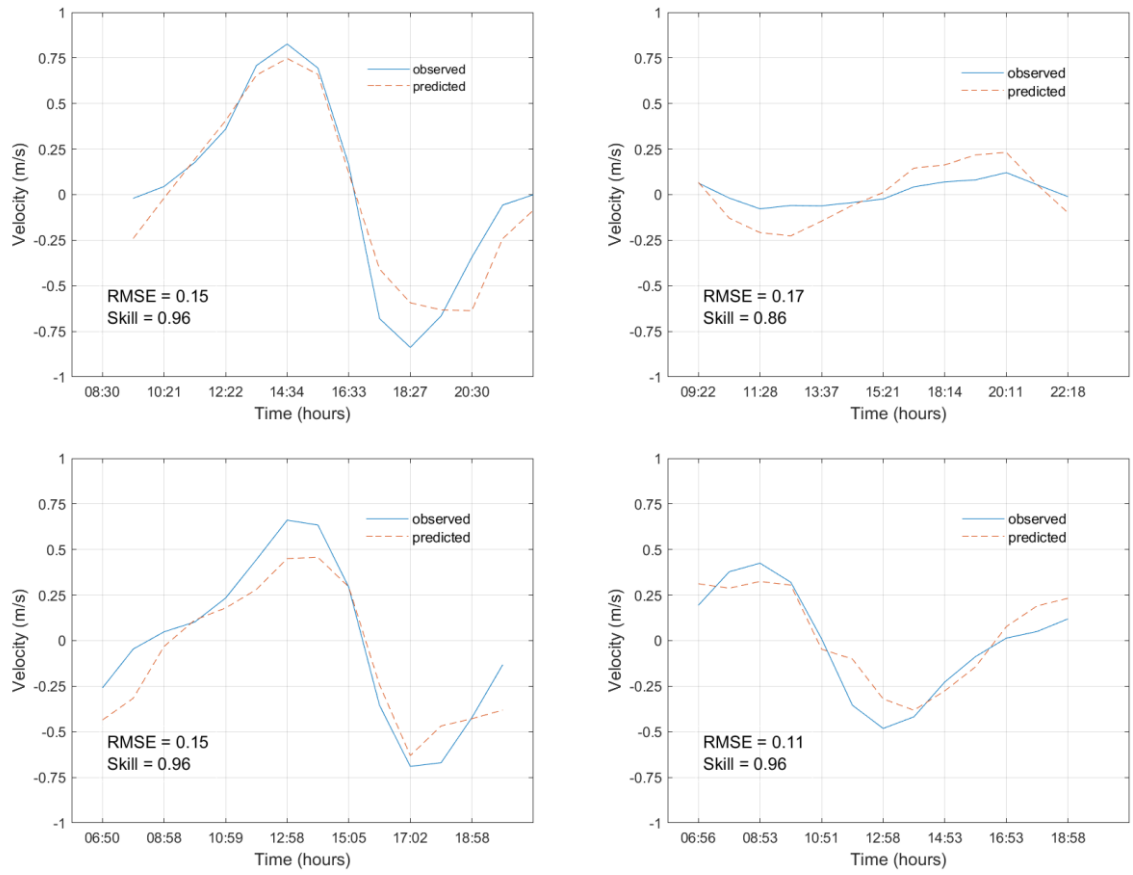


Figure 4.6. Modelled depth-averaged current velocities vs observed depth-averaged current velocities for the Faro-Olhão Inlet in spring (upper left) and neap tide (right) and for the Armona Inlet in spring (bottom left) and neap tide (bottom right). RMSE and Skill are provided for all data.

## 4.2. Structured grid model setup

### 4.2.1. Basic setup

The morphological effects of SLR in the evolution of the tidal channels were simulated with a structured grid modelling approach previously used by Gonzalez-Gorbeña et al. (2018). The baseline model was developed in the Delft3D-FLOW domain, with a morphological model coupled to a hydrodynamic model following a 2D depth averaged approach (Lesser et al., 2004). The domain for this study extends from Tavira island up to the western limit of Ancão

Peninsula, reaches approximately 6 km offshore and exceeds 35 km in the alongshore direction (middle-western part of Ria Formosa lagoon, Fig. 4.7). The average cell size ranges from 750 x 175m offshore, to 20 x 10 m at the inner channels and inlets, where the grid has been refined in comparison to that used by González-Gorbeña et al. (2018). Local bathymetry was based on LiDAR data from 2011 and bathymetric surveys from 2016 (SCORE project, see Gonzalez-Gorbeña et al., 2018).


4.7. Refined grid used in the structured model approach. The grid cells of the Faro-Olhão and Ancão inlets are slightly more refined (Source: "Western Ria Formosa". 36.980414º N and 7.884412º W. Google Earth. December 31st, 2011. Retrieved September 25th, 2020)

The model was forced with an offshore water level boundary and two lateral water level gradient boundary conditions (Neumann boundaries). Astronomical forcing consisted of the M2 tidal component, an amplitude correction for the M2 component and a schematized tide based on tidal asymmetry between the main diurnal (O1 and K1) and semidiurnal (M2) tidal components. The main local tidal constituents were derived from the TPXO global tidal model (Egbert and Erofeeva, 2002). Waves and wind were not modelled for this study, as they are of minor influence inside the lagoon (Gonzalez-Gorbeña et al., 2018). The schematized tide was applied to represent a full year astronomical tide in combination with the use of a morphological acceleration factor (Morfac, see Lesser et al., 2004), by producing similar residual transport and morphological evolution (Lesser, 2009).

### 4.2.2. Selection of modelling parameters

Some parameters of the baseline model (calibrated and validated by Gonzalez-Gorbeña et al., 2018) were adjusted to better suit the present research focus (Table 4.4). A value of Morfac of 100 was compared to the original Morfac value of 48 used in the baseline model, using sensitivity runs of 12 and 25 years. No significant differences were found between the simulations, and a Morfac of 100 was selected for the final setup to save computational time. Bottom friction values were adjusted from a White-Colebrook formulation to Manning coefficient values (based on values provided by the results of Kfjerve et al, 1991; Lawrence et al., 2004; and Temmerman, 2012, among others). Different Manning coefficient values were assigned to sea, land, main tidal channels, tidal inlets and salt marshes (Table 4.5) and a sensitivity test (run for a 25 year simulation period and a Morfac of 100) was performed to select the optimal Manning coefficient values for this study. This modification of roughness input was found more adequate than applying a White-Colebrook coefficient. Finally, in the baseline model the median sediment size (D50) was assumed as 425 μm, based in measurements in the inlets and flood deltas by Pacheco et al. (2011); however, this value might be inadequate to represent tidal flats and tidal channels, as measurements of boreholes taken in the tidal channels show a mean grain size range of 53-218 μm (Sousa et al., 2019). Additional sediment size scenarios were tested (one run with a grain size with D50 = 64 μm, another run set for D50 = 175 μm, and a third run combining the two sediment fractions) by K. van den Hoven (Carrasco et al., 2019).

Table 4.4. Original model configuration and current model configuration.

| Model setup parameters | González-Gorbeña et al. (2018) | Current model configuration |
|---|---|---|
| ***Grid:*** | | |
| Spacing | 462 x 1100 M x N | 450 x 1509 M x N |
| Resolution Δx Δy – offshore | 750 x 175 m | 750 x 175 m |
| Resolution Δx Δy – inlets | 20 x 15 m | 20 x 10 m |
| ***Numerics:*** | | |
| Threshold depth | 0.1 m | 0.1 m |
| Marginal depth | -999 m | -999 m |
| Smoothing time | 60 min | 60 min |
| ***Physics:*** | | |
| Gravitational acceleration | 9.81 $m/s^2$ | 9.81 $m/s^2$ |
| Water density | 1000 $kg/m^3$ | 1025 $kg/m^3$ |
| Roughness formula | White-Colebrook | Manning ($s/m^{1/3}$) |
| Uniform horizontal eddy viscosity | 2 $m^2/s$ | 2 m /s |
| Uniform horizontal eddy diffusivity | 10 $m^2/s$ | 10 $m^2/s$ |
| Morphological acceleration factor (Morfac) | 48 | 100 |
| Min. depth sediment calculation | 0.1 m | 01 m |
| Van Rijn ref height | 0.5 | 0.5 |
| Threshold sediment thickness | 0.05 m | 0.05 m |
| ***Sediment type:*** | | |
| Cohesive | No | No |
| D50 | 425 µm | 175 µm |
| Specific density | 2650 $kg/m^3$ | 2650 $kg/m^3$ |
| Dry bed density | 1600 $kg/m^3$ | 1600 $kg/m^3$ |
| Initial layer thickness at bed | 5 m | 5 m |
| ***Time:*** | | |
| Spin-up time 1440 (min) | 1440 min | 1440 min |
| Timestep | 0.5 min | 0.5 min |
| Time frame | 8.5 days | 92.25 days |
| ***Output format:*** | | |
| Restart interval | 0 min | 132840 min |
| Map interval | 60 min | 5760 min |
| History interval | 10 min | 1440 min |

Table 4.5. Values of Manning's n tested for different areas of the lagoon. The central column showcases the values chosen for all further simulations.

| **Areas of the lagoon** | **Manning n values tested** | | | | |
|---|---|---|---|---|---|
| **Offshore** | 0.05 | 0.05 | 0.05 | 0.05 | 0.05 |
| **Land** | 0.05 | 0.05 | 0.05 | 0.05 | 0.05 |
| **Tidal inlets** | 0.025 | 0.35 | 0.1 | 0.2 | 0.1 |
| **Tidal channels** | 0.05 | 0.35 | 0.3 | 0.1 | 0.1 |
| **Salt marshes** | 0.03 | 0.35 | 0.4 | 0.3 | 0.2 |

After the sensitivity analysis, the adjusted model was used to simulate longer time periods. No further calibration or validation processes were performed due to time constraints, which introduces a degree of uncertainty in the model that must be noted when analysing the results. A new baseline model was defined with a Morfac value of 100 and a D50 of 175 μm. Simulations were conducted for 89 years since the starting year 2011. To simulate the evolution from 2011 until 2100, four subsequent simulations were computed. The first three runs simulated 25 years each and the final run simulated 14 years (timesteps from 0-25, 25-50, 50-75 and 75-89 years). Local bathymetry was updated at the beginning of each simulation. The conducted simulations enclosed a simulation time frame of 92.25 days (~92 days, approximately three months). Average computation time for the total 89-year scenarios was 33 days.

## 4.3. Sea-Level Rise scenarios

To study the effects of SLR in the long-term hydrodynamics of the Ria Formosa, four SLR scenarios were applied to the unstructured model after calibration and validation.

The first imposed scenario, SLR= 0.47 m, corresponds to the projected regional Relative Sea-Level Scenario (RSLR) for the year 2100, provided by Antunes and Taborda (2009) who calculated it by using the Cascais tide gauge. The second and third SLR scenarios, SLR= 0.53 m and 0.74 m, reflect the Global Mean Sea Level expected for 2100, for the scenarios RCP 4.5 and RCP 8.5, respectively, reported by the 5th Assesment Report of the IPCC (2014). The fourth and highest SLR scenario so far (dubbed as Extreme), SLR= 0.84 m, corresponds to the GMSL value of the High-End projection of Jackson and Jevrejeva (2016), which considers a high contribution of the land-ice component not modelled in most of the papers featured in the IPCC. To simulate each SLR scenario an additional A0 tidal constituent, incorporating the

projected SLR values (with fixed amplitude equal to the SLR value and no phase), was added along to the astronomic sea boundary (the A0 constituent simply applies a constant vertical shift to the portrait water levels at the sea boundary) in each simulation (i.e. SLR scenario). The results of the SLR simulations were analysed assuming no morphological feedback and were compared with the results of a simulation without SLR (Baseline).

For the structured grid model only one SLR scenario was chosen to be applied due to time constraints. A SLR rate of 0.98 m (higher than the SLR scenarios for the unstructured grid model) was applied to assess morphological changes; this scenario corresponds to the highest value among the likely range of SLR of the RCP 8.5 scenario presented by the IPCC for the year 2100 (5th Assessment Report of the IPCC, 2014). To simulate the SLR scenario, a linear SLR rate of 1.1 mm/year was incorporated to each of the model simulations (0-25, 25-50, 50-75 and 75-89 years) as an additional bc0 file (a time series file that applies a correction to the simulated flow boundary conditions).

## 4.4. Data analysis

### 4.4.1 Unstructured grid model results analysis

The analysis of the unstructured model results was made by comparing tide propagation asymmetry and current velocity asymmetry induced by the newly SLR scenarios along the Faro, Ramalhete and Ancão channels, and on the Faro-Olhão, Ancão and Armona inlets. The harmonic constants of the main tidal constituents were determined using the T-TIDE package (Pawlowicz et al., 2002). To explore the variation of the different variables with the distance to the Faro-Olhão Inlet (the main water exchange inlet between the lagoon and the ocean), a series of observation points and cross-sections (Figure 4.8) were modelled at various locations. A minimum of 3 observation points and 2 cross-sections per channel, with an interval of 1.5 km between each point/cross-section, was considered adequate to consider the modelled results as representative of the hydrodynamics in the area. Additionally, 3 cross-sections were modelled in the Faro-Olhão, Ancão and Armona inlets to address the changes in current velocity under different SLR scenarios at the entrances of the coastal lagoon.

To explore the changes in the strength of tidal asymmetry and flood/ebb dominance under the different SLR scenarios, three mathematical conditions were calculated and analysed: (i) the ratio between the harmonic tidal components M4 and M2 (M4/M2); (ii) the phase difference between twice the M2 component phase and the M4 component phase (2M2-M4;

Guo et al., 2014), (iii) and the average ratio between the duration of rising and falling tide (Rt (1); Stark et al., 2017), determined by:

$$Rt = \frac{1}{n}\sum_{j=1}^{n} \left(\frac{T_{rising}(j)}{T_{falling}(j)}\right) \quad (1)$$

where n is the total amount of tides in the simulation, j represents an individual tide, and $T_{rising}$ and $T_{falling}$ are the total duration of water level rise and fall, respectively.

The M4/M2 ratio reflects the strength of the tidal asymmetry, while 2M2-M4 and Rt reflect the direction of the residual sediment transport; 2M2-M4 and Rt are calculated as complementary conditions due to the differences in their approach, with 2M2-M4 using harmonic tide components and Rt using the duration of the rising and falling tides. Following the Guo et al. (2014) approach, a phase difference between 0 and 180º in the 2M2-M4 parameter indicates a flood dominance in the tidal asymmetry, and a phase difference between 180 and 360º indicates ebb dominance. Following the Stark et al. (2017) approach, a value of Rt < 1 indicates flood dominance and Rt > 1 indicates ebb dominance. The harmonic constants of the main tidal constituents used for the M4 overtide and 2M2-M4 were determined using the T-TIDE package (Pawlowicz et al., 2002) and a full month of modelled data, and the Rt mathematical condition was calculated using a full month of modelled data as well. Maximum current velocity values and current velocity averages for a full month of modelled data were represented, with positive values (current velocity > 0 m/s) indicating maximum velocities during the flood period and negative values (current velocity < 0 m/s) indicating maximum velocities during the ebb period.

### 4.4.2 Structured grid model results analysis

The analysis of the structured grid model results was made by comparing elevation differences, bathymetry exchange rates and channel displacement induced by the applied SLR along the Faro, Ramalhete and Ancão tidal channels, along the surrounding salt marsh flats and on the Faro-Olhão and Ancão inlets. A series of observation points were modelled in locations similar to the observation points modelled in the unstructured grid model configuration, to compare the resulting predictions and slightly reduce the uncertainty expected by the lack of calibration and validation of the structured grid model. To observe erosion and accretion throughout the lagoon, the starting 2011 bathymetry was subtracted from the final bathymetry (year 2100). Elevation differences between the bathymetry of the Baseline (no SLR) and the SLR scenario over time were represented for the final bathymetry

of each of the conducted simulations (at 25, 50, 75 and 89 years). A range of -2 m to 2 m of elevation differences, with differences stronger than 2 m grouped together, was considered adequate to assess possible future morphological changes induced by SLR; this range was selected with the intention of identifying the areas more likely to be affected by SLR and reduce the influence of strange elevation difference peaks found in the results (likely to be misrepresentations of the model due to the lack of calibration and validation).

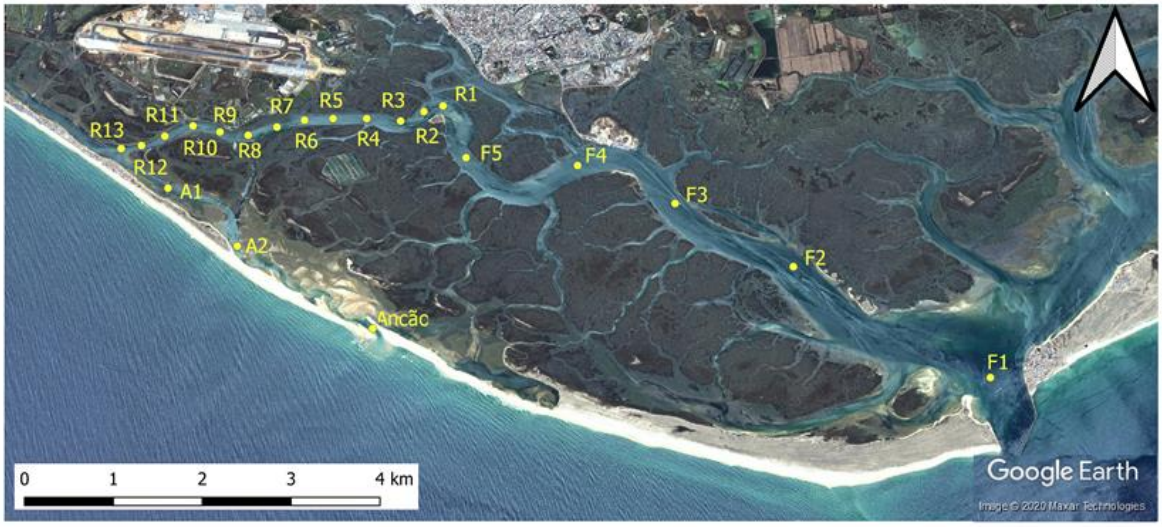


Figure 4.8. Location of the twelve observation points (yellow circles) modelled around the Ria Formosa. (Source: "Western Ria Formosa". 36.980414º N and 7.884412º W. Google Earth. December 31st, 2011. Retrieved September 25th, 2020)

To specifically assess morphological changes over time, a series of cross-sections were modelled in the aforementioned channels and inlets (with a minimum interval between cross-sections of ~ 0.4 km for the Ramalhete Channel and a minimum interval of ~1.5 km for the rest of the areas). Cross-sectional depth profiles were obtained using the depth files at the end of each of the simulations. To keep consistency and enable comparison between the two models, observation points and cross-sections were modelled in the exact locations as the ones in the unstructured grid modelling approach. This could not be achieved for all cross-sections because cross-sections in the structured grid approach can only be modelled along the cells limits, unlike in the unstructured grid approach. Nevertheless, the modelled cross-sections were considered adequate to represent the morphological evolution of Ria Formosa. Maximum cross-section bathymetry exchange rates were calculated for each cross-section. Rates were calculated for the entire simulation period, as well as for each of the timesteps simulated (0-25, 25-50, 50-75 and 75-89 years), by subtracting the original maximum depth

of a channel from the new maximum depth, and dividing it by the total number of simulated years. Tidal channel displacement induced by SLR was studied by using the location of maximum channel depth within a cross-section. The distance along a cross-section between the location of maximum channel depth and the side of the channel was calculated to observe displacement over time.

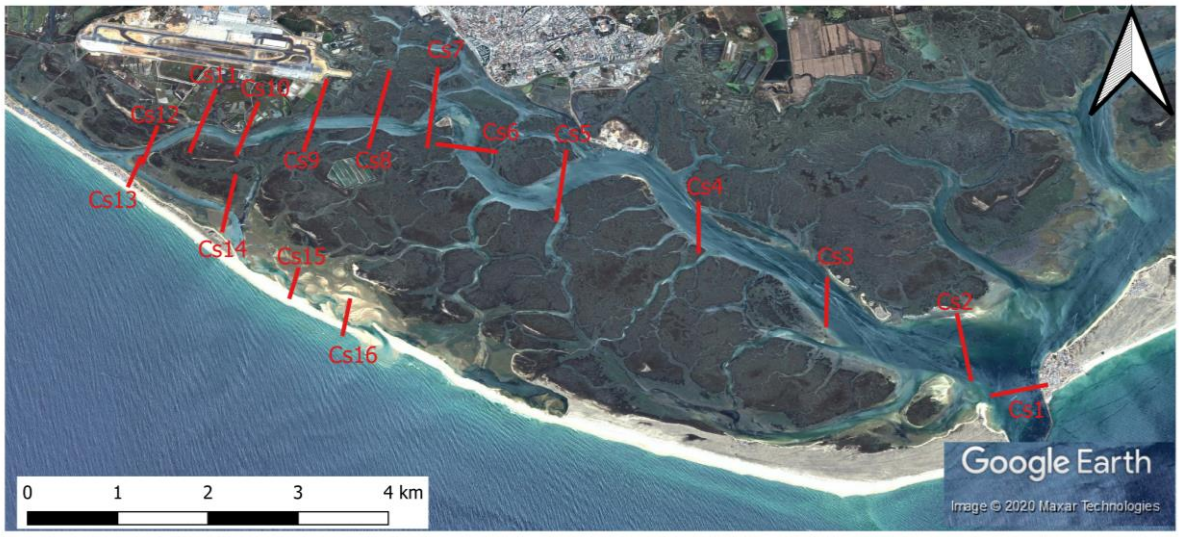


Figure 4.9. Location of the cross-sections (red lines) used for the long-term morphological evolution simulations. (Source: "Western Ria Formosa". 36.980414º N and 7.884412º W. Google Earth. December 31st, 2011. Retrieved September 25th, 2020)

# Chapter 5: Results

## 5.1. Hydrodynamic results (Unstructured model approach)

### 5.1.1 Tidal asymmetry under SLR

The values of the surface amplitude ratio (M4/M2 ratio) were calculated for the Baseline scenario (no SLR) and the four modelled SLR scenarios (Figure 5.5). The Baseline scenario shows an increase of the M4/M2 ratio, and therefore an increase in the tidal asymmetry strength, with the distance to the Faro-Olhão Inlet. After Obs9, however, there is a decrease in the values of the M4/M2 ratio, followed by another increase from Obs11 to Obs12.

This pattern is modified under the different SLR scenarios. Under the RSLR and RCP 4.5 scenarios, the values of the M4/M2 ratio increase until Obs6, decrease from Obs6 to Obs9, and increase again for all stations after Obs9 (Figure 5.1). Under the RCP 8.5 scenario and the Extreme scenario, the M4/M2 ratio values increase up to Obs5, decrease from Obs5 to Obs8 (RCP 8.5 scenario) and Obs7 (Extreme scenario) and increase thereafter. Higher SLR rates cause a reduction in the values of the M4/M2 ratio for most observation points, with Obs8 to

Obs11 showing different responses. Obs8 to Obs10 show a decrease in tidal asymmetry strength with SLR, followed by a progressive increase under higher SLR rate scenarios (scenario RSLR for Obs10, scenario RCP 4.5 for Obs9 and scenario RCP 8.5 for Obs8); Obs11 shows a progressive increase of tidal asymmetry strength with higher SLR rates.

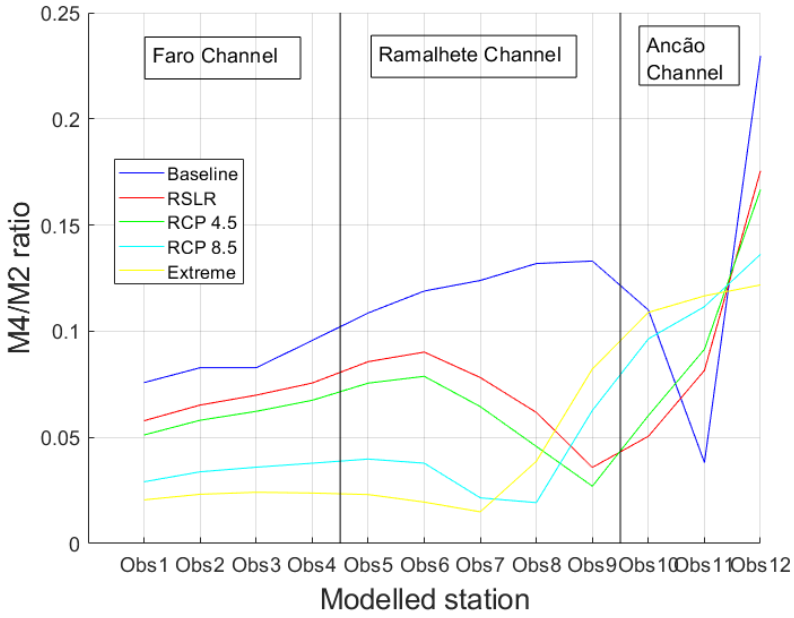


Figure 5.1. Modelled strength of the M4/M2 ratio for the different SLR scenarios in the Faro, Ramalhete and Ancão channels.

For the Baseline scenario, both the 2M2-M4 phase difference and Rt flooding/falling tide ratio show ebb dominance (2M2-M4 > 180º, Rt > 1) in the tidal asymmetry for most of the stations, with a shift to flood dominance (2M2-M4 < 180º, Rt < 1) in stations Obs11 and Obs12 (located at 15 and 16.5 km from the Faro-Olhão Inlet) (Figure 5.2).

With SLR, the stations in which the shift from ebb to flood dominance occurs are altered based on the rate of SLR applied. Under the lowest SLR applied (RSLR scenario), the shift from ebb to flood dominance appears closer to the FO Inlet than in the Baseline scenario (no SLR), moving from Obs11 to Obs10 (2M2-M4) and from Obs11 to Obs9 (Rt), located at 13.5 km and 12 km from the FO Inlet, respectively (Figure 5.2). Under the highest SLR rate applied (Extreme scenario) the shift is moved much closer to the FO Inlet compared to the Baseline scenario, moving from Obs11 to Obs7 (15 km to 9 km from the FO Inlet) for both 2M2-M4 and Rt.

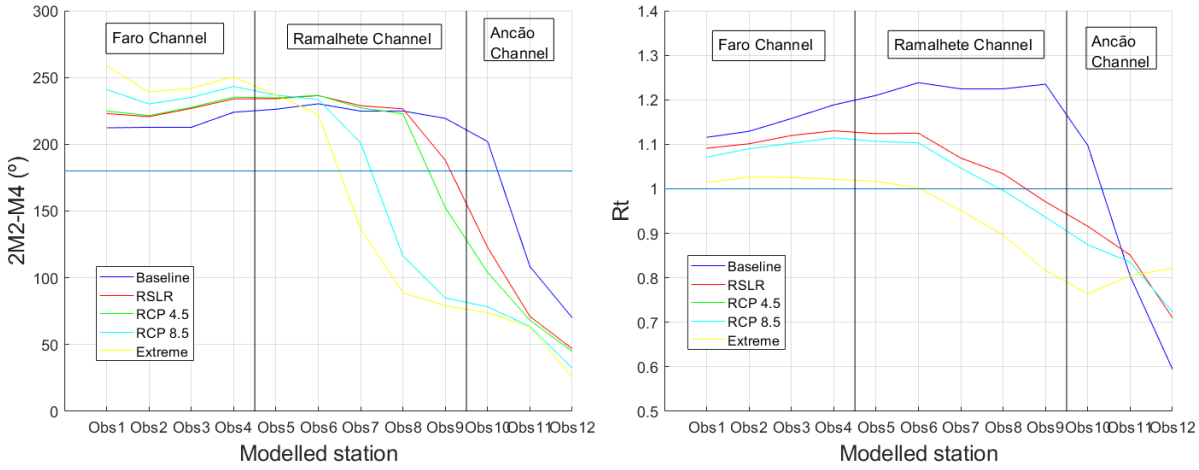


Figure 5.2. Modelled phase differences of the M2 and M4 components (2M2-M4, left) and ratio between duration of rising and falling tide (Rt, right) for the different SLR scenarios in the Faro, Ramalhete and Ancão channels. The horizontal blue lines mark the separation between ebb and flood dominance: the 180º value (left) and the 1 value (right).

### 5.1.2 Average and maximum current velocities under SLR

Under the Baseline scenario (no SLR), all cross-sections delimited in the main channels show positive average current velocity values, reflecting flood dominance (Figure 5.3). This is not the case in the cross-sections delimited in the inlets, in which the average velocity values are positive for the Faro-Olhão and Ancão inlets, but negative (ebb-dominant) for the Armona Inlet. Under the hydrodynamic conditions imposed by the different SLR scenarios, the average current velocity values are slightly lowered in most of the cross-sections delimited in the main channels, with a small maximum reduction of ~0.05 m/s in current velocity in Cs8. However, the average velocity values seem to increase in cross-sections Cs10 and Cs11 (Figure 5.3). The effects of SLR are also shown in the inlets, where the average current velocity values slightly decrease in the Faro-Olhão Inlet and increase in both the Ancão and Armona inlets. The average current velocity values of the latter also change from negative (ebb dominant) to positive (flood dominant) under the RCP 8.5 and Extreme scenarios, even if they always stay very much near zero.

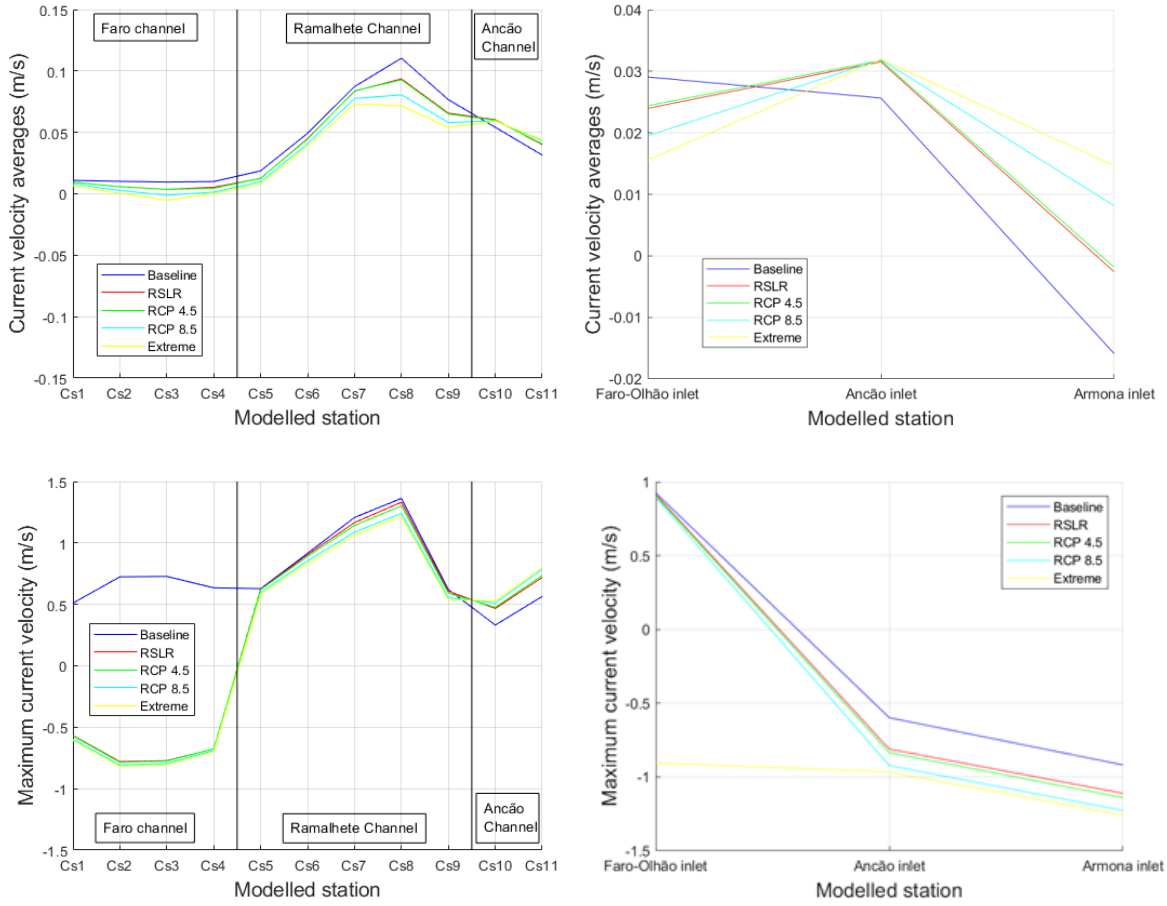


Figure 5.3. Modelled current velocity averages (upper row) and maximum current velocity (lower row) for the different SLR scenarios in the three channels and the Faro-Olhão, Ancão and Armona inlets. Positive average values indicate flood dominance and negative values indicate ebb dominance. Positive maximum values indicate maximum velocity during flood and negative maximum values indicate maximum velocity during ebb.

Under the Baseline scenario, the cross-sections delimited in the main channels and the Faro-Olhão Inlet show positive maximum velocity values (flood dominance), while the ebb-dominant Ancão and Armona inlets show negative maximum velocity values. SLR affects the cross-sections delimited in the main channels differently; it decreases maximum current velocities in all cross-sections but Cs10 and Cs11 (the two closest to the Ancão Inlet), and in the case of cross-sections Cs1 to Cs4, current velocities shift from reaching their maximum value during the flood period to the ebb period (Figure 5.3). Among the inlets, the Faro-Olhão Inlet shows negligible changes in maximum current velocity under all SLR scenarios except for the Extreme scenario, where the current reaches maximum velocity values in the ebb period instead of in the flood period. The maximum current velocities in the Ancão and Armona inlets increase with SLR, with the current reaching maximum velocity in the ebb period for both inlets (Figure 5.3)

## 5.2. Morphodynamic results (Structured model approach)

### 5.2.1. Bathymetric changes in western Ria Formosa

It is important to stress that calibration and validation were not performed for the structured model approach, which requires a greater attention when discussing the results to avoid exaggerated claims. Bathymetric changes in the westernmost sector of the Ria Formosa, after 89 years of simulation and for the Baseline scenario, are shown in Figure 6.1. A maximum range of 2 meters (equivalent to a 20 mm/year bathymetry exchange rate) was selected when analysing bathymetry changes, to avoid the influence of unrealistically high erosion or sedimentation values (e.g. a value of 10 m of sedimentation surrounded by much smaller values). Bathymetry exchange rates lower than 1 mm/year were considered too low to produce noteworthy differences.

Under the Baseline scenario, small accretion and erosion patches (ranging between ~0.2 and 0.5 m) can be seen in the salt marsh area between the Faro and Olhão channels (Figure 6.1). Bathymetric changes are higher in areas close to the inlets, with the Ancão Inlet showing patches of accretion and erosion of ~1 m. The biggest changes are seen in the entrance of the Olhão Channel: a central patch of strong accretion (higher than 2 m) can be seen in the mouth of the Olhão Channel, surrounded by a patch of light accretion (in the range of 0.3 to 1 m) in the tidal delta of the Faro-Olhão Inlet, and by a long patch of strong erosion (higher than 2 m) that reaches into the Olhão Channel (Figure 6.1).

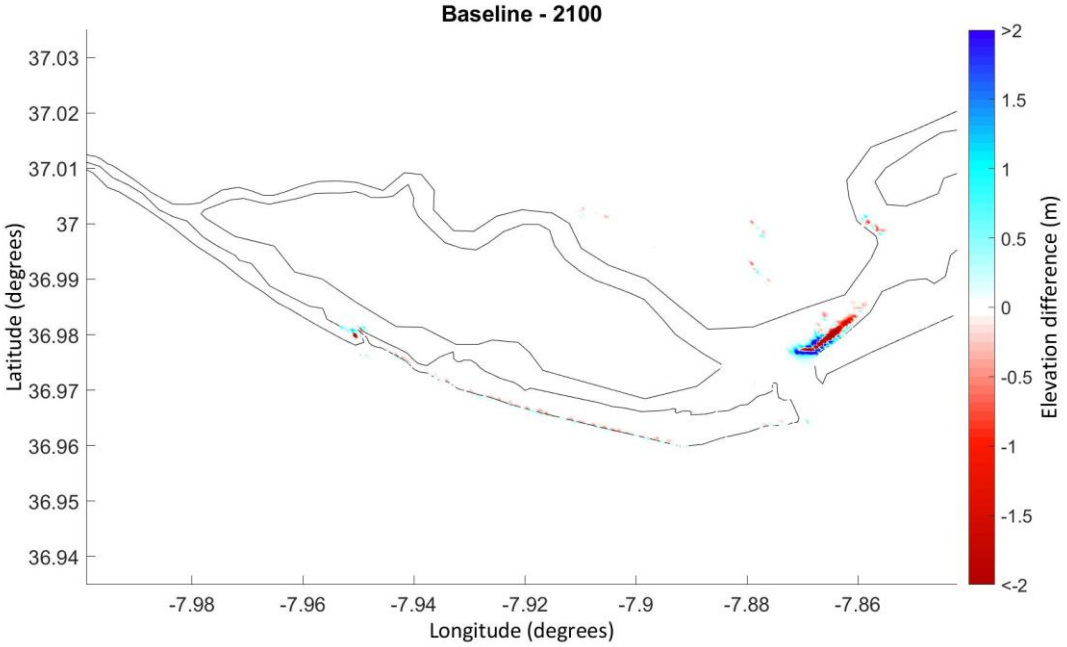


Figure 6. 1. Bathymetric evolution of the study area, after 89 years and for the Baseline scenario. Accretion is shown in blue and erosion in red.

Under the SLR scenario strong accretion and erosion (close to or higher than 2 m) appear in a wide area, including the previously defined patches located in the entrance of the Olhão Channel (Figure 6.2). The Ancão Inlet shows stronger accretion over a wider area under SLR, and a new patch of accretion higher than 2 m appears in the mouth of the Faro-Olhão Inlet. Accretion and erosion patches ranging between ~0.2 and 0.5 m appear again in the salt marsh area between the Faro and the Olhão channels, albeit in different locations. Finally, sporadic/patchy erosion of ~0.3 m can be seen in the salt marsh area between the Faro, Ramalhete and Ancão channels.

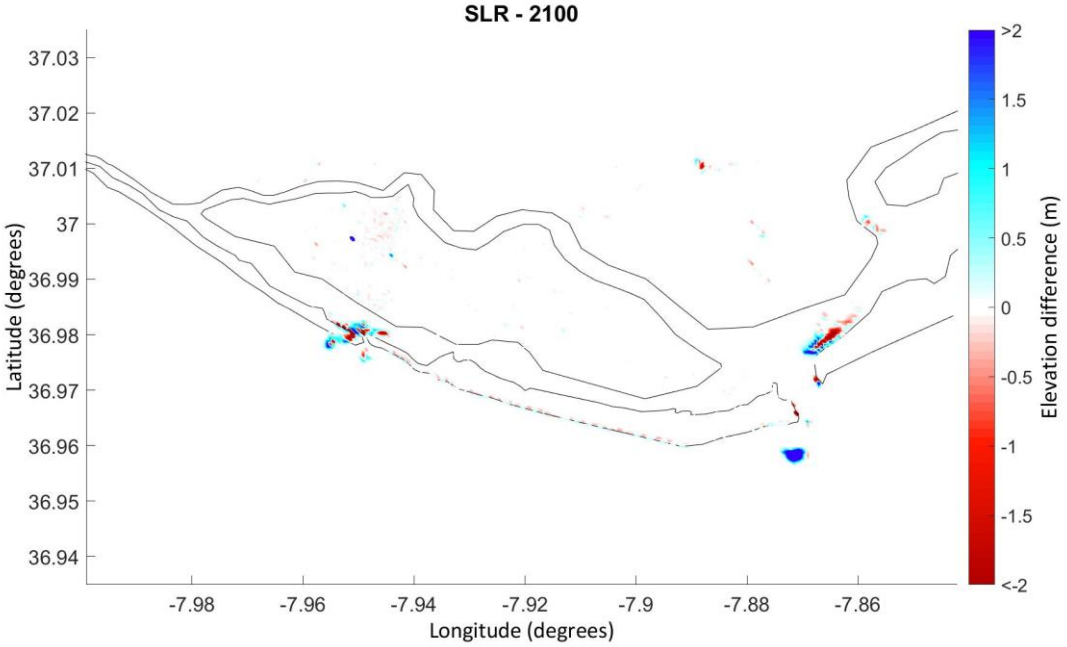


Figure 6.2. Bathymetric evolution of the study area, after 89 years and for the SLR scenario. Accretion is shown in blue and erosion in red.

### 5.2.2 Bathymetric changes in the Ramalhete Channel

The effect of SLR in bathymetric changes in the Ramalhete Channel and the neighbouring areas and the effect of SLR in cross-sectional bathymetry profiles were explored in this study. No bathymetric changes were seen under the Baseline scenario, even after the full simulation period (Figure 6.3). Bathymetric changes are, however, observed when SLR is applied: after 25 years small and sporadic erosion, in the range of 0.1 m, appears in the salt marsh area between the channels and in the margins of the Ramalhete Channel (Figure 6.4). After 50 years slightly more erosion patches appear, with similar values to those seen after 25 years. In the next timestep simulated (75 years) several more patches of erosion appear, with values in the range of 0.1 to 0.3 m. Some accretion patches with values of ~0.1 m also appear, surrounding the erosion patches (Figure 6.4). Finally, after 89 years of simulation, patches of accretion with values up to 2 m or higher appear. No other future bathymetric changes can be seen, with the erosion and accretion patches following the distribution seen after the 75 years timestep (Figure 6.4).

Figure 6.3. Long-term bathymetric evolution of the Ramalhete Channel and its surroundings under the Baseline scenario. The four timesteps (25, 50, 75 and 89 years) simulated are shown chronologically from top to bottom. Accretion is shown in blue and erosion in red.

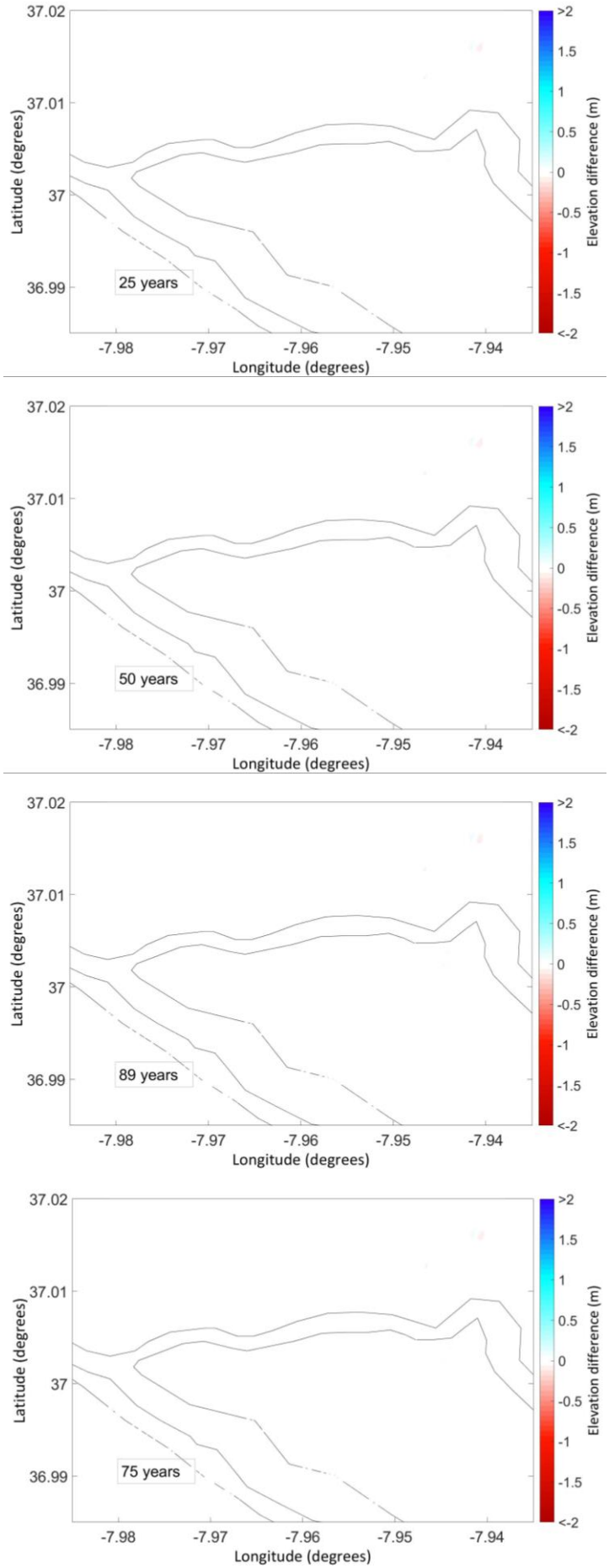

Figure 6.4. Long-term bathymetric evolution of the Ramalhete Channel and its surroundings under the SLR scenario. The four timesteps (25, 50, 75 and 89 years) simulated are shown chronologically from top to bottom. Accretion is shown in blue and erosion in red.

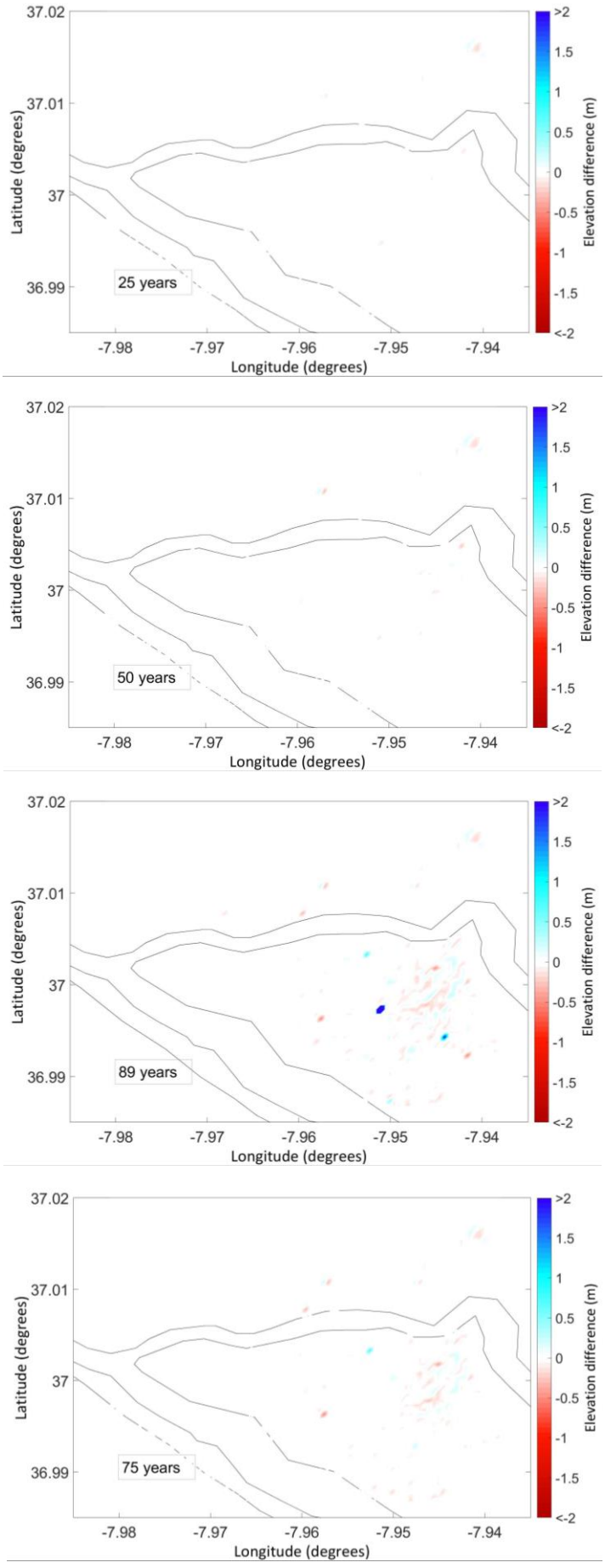

The analysis of the cross-section bathymetry profiles shows a minimal impact of SLR in the bathymetry of the Ramalhete Channel, with all cross-sections except one (Cs16) showing negligible bathymetric changes. Under the SLR scenario, Cs16 appears to show some sedimentation in the channel margins and some erosion in the bottom of the channel, with values between 0.2 and -0.3 m respectively (Figure 6.5). Bathymetry exchange rates for all cross-sections under both scenarios were calculated, for the full time period simulated (89 years) and for each of the four timesteps simulated (0 to 25 years, 25 to 50 years, 50 to 75 years and 75 to 89 years; Table I.1). Most bathymetry exchange rate values are very low for all cross-sections and timesteps analysed (Table 6.1); however, this is not the case for CS16. Cs16 shows a maximum erosion rate under the Baseline scenario of -3.4 mm/year for the full time period; the highest bathymetry exchange values are found under the SLR scenario, with a maximum accretion rate of 19.4 mm/year between the 50 and 75 years simulations and a maximum erosion rate of -57.5 mm/year between the 75 and 89 years. The maximum depth points location under the SLR scenario do not change throughout the timesteps, with channel displacement absent for all cross-sections.

Table 6.1. Bathymetric exchange rates in mm/year for the different bathymetry profiles simulated in this study. Only timesteps with exchange rates higher than 1 mm/year are shown.

| | **Baseline scenario** | **SLR scenario** | | |
|---|---|---|---|---|
| **Cross section** | **0-89 years** | **50-75 years** | **75-89 years** | **0-89 years** |
| **1** | 0.05 | -0.01 | 6.08E-04 | 0.14 |
| **6** | 1.16E-07 | 2.07E-07 | 3.69E-07 | 0 |
| **7** | 3.93E-05 | 6.79E-05 | 1.21E-04 | 7.22E-06 |
| **8** | 2.68E-05 | 4.78E-05 | 6.42E-05 | 0 |
| **9** | 1.71E-05 | 4.23E-05 | 3.35E-05 | -9.98E-15 |
| **10** | 5.71E-06 | 1.03E-05 | 1.76E-05 | 0 |
| **11** | 1.66E-05 | 6.36E-06 | 9.37E-05 | 1.18E-11 |
| **13** | -9.27E-11 | -9.44E-11 | -1.69E-10 | 3.36E-11 |
| **14** | 2.42E-05 | 5.99E-10 | 1.5E-04 | -9.61E-12 |
| **15** | 0.08 | 0.07 | 0.41 | 6.94E-13 |
| **16** | -3.44 | 19.4 | -57.5 | 2.97E-03 |

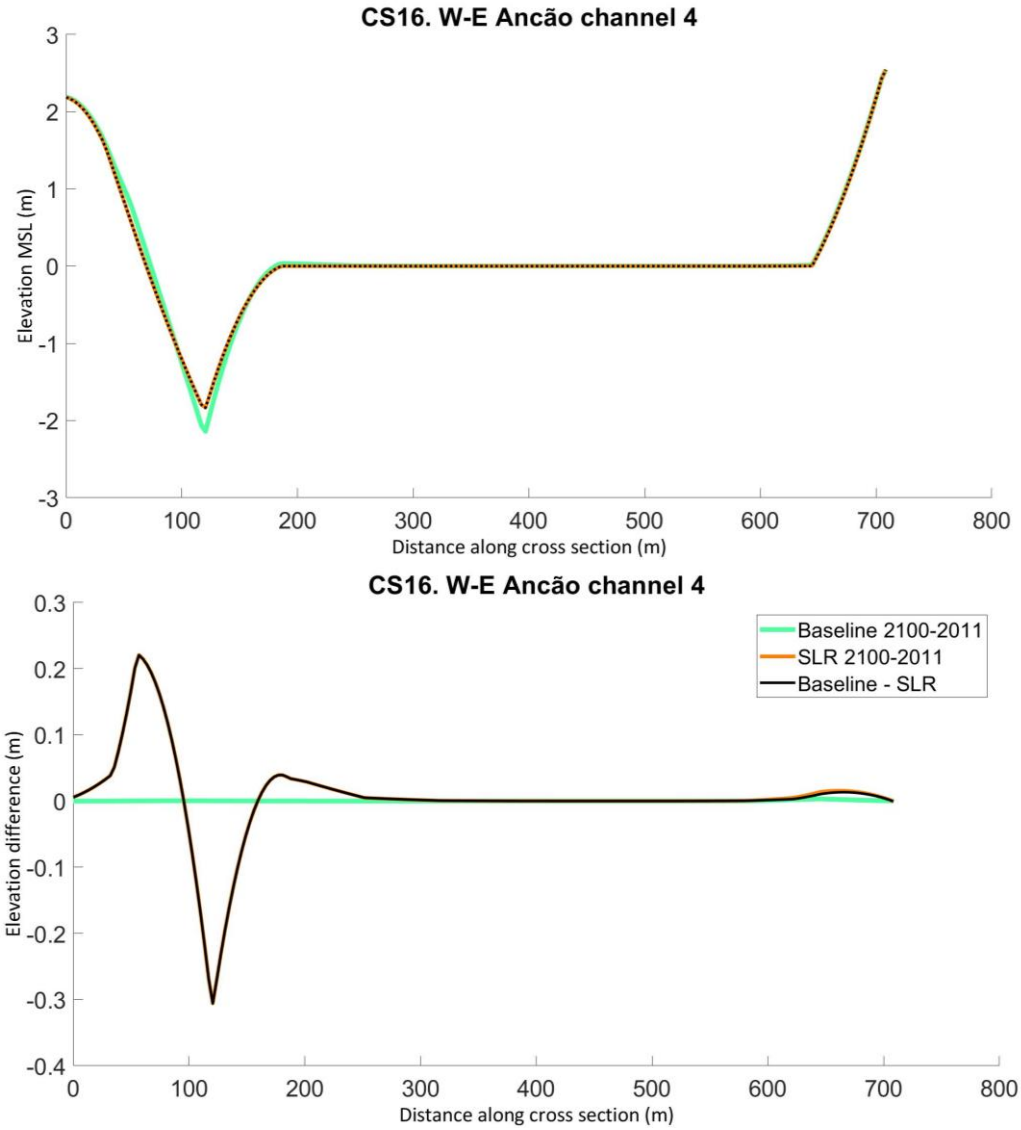


Figure 6.5. Channel bathymetry (upper graph) and elevation differences between scenarios (lower graph) in Cs16. Positive values in elevation differences indicate accretion and negative values indicate erosion.

# Chapter 6: Discussion

## 6.1. Tidal response under SLR

To assess the impact of SLR in tidal asymmetry along the tidal channels, an evaluation of changes in tidal asymmetry strength (M4/M2 ratio), phase difference of the M2 and M4 components (2M2-M4) and flooding/falling tide ratio (Rt) is presented in this study. The unstructured model results show that the response of tidal asymmetry to SLR is not equal in all areas of the system. Overall SLR causes a decrease in tidal asymmetry strength, and therefore a decrease in the strength of the flood/ebb dominance; however, the observation points located

between Obs7 (located in the middle area of the Ramalhete Channel) and Obs10 (located in the western section of the Ancão Channel) show differing responses with increasing tidal asymmetry strength under specific SLR rates (Figure 5.1). In this area, the number of stations shifting from ebb to flood-dominance appears to be influenced by the rate of SLR simulated; under the lowest SLR rate scenario (RSLR), SLR seems to enhance flood-dominance only in Obs10, and under the highest SLR rate scenario (Extreme), SLR seems to enhance flood-dominance in four stations (Obs7 to Obs10; Figure 5.2). SLR-induced changes in local intertidal characteristics (e.g. intertidal storage capacity and/or bottom friction of tidal flats; Friedrichs and Aubrey, 1994; Fortunato and Oliveira, 2005; Stark et al., 2017) are likely to be the reason for the enhancement of flood-dominance; when SLR is not applied, only the two stations located closer to the Ancão Inlet show flood-dominance (Figure 5.6). The obtained results are in agreement with those of Stark et al. (2017), who modelled the impact of intertidal area characteristics in the hydrodynamics of the Scheldt estuary and found that tidal flats located low in the tidal frame enhance flood dominance.

Under SLR, the results of the tidal asymmetry indicators are qualitatively similar, although Rt seems to favour the flood-dominance behaviour in comparison to 2M2-M4. Regardless of the considered indicator, the shifts between ebb-dominance and flood-dominance seem to be related to the distance to the Ancão Inlet; as higher SLR rates are applied, flood-dominance is seen in stations further and further from the Ancão Inlet, reaching into the Ramalhete Channel (Figure 5.2). This seems to imply that the role of the Ancão Inlet in the type of tidal asymmetry observed increases with SLR. In a multiple inlet system, the inlet that captures a higher tidal prism determines the overall flood or ebb-dominance of the bay (Pendleton and Fitzgerald, 2005). In the Ria Formosa, the flood-dominated Faro-Olhão Inlet captures most of the tidal prism of the lagoon (~61% in spring tides and ~45% in neap tides) and the Ancão Inlet has a reduced importance compared to the Faro-Olhão and Armona inlets, capturing only ~8% of the total flow in spring tides and ~5% in neap tides (Pacheco et al., 2010). The Ancão, Faro-Olhão and Armona inlets show strong nonlinear hydrodynamic interdependence, which contributes to the stability of the inlets; conversely, this interdependence means that changes in the hydrodynamic properties of an inlet not only affect the specific inlet, they also affect the other inlets (Salles et al., 2005). Therefore, SLR seems to induce changes in the hydrodynamic equilibrium of the Ria Formosa, potentially increasing the general importance of the Ancão Inlet and reducing the importance of the other inlets.

Changes in average current velocities induced by SLR were mostly negligible, with differences smaller than 0.05 m/s. However, it must be noted that the average current velocity

values of the Armona Inlet change from negative (velocity recorded during ebb period) to positive (velocity recorded during flood period) (Figure 5.3). The impacts of SLR are more relevant in the maximum velocity current values, with velocity changes higher than 0.1 m/s (Figure 5.3). Maximum velocity values of stations Cs1 to Cs5 shift from positive to negative under all SLR scenarios; this also occurs in the Faro-Olhão Inlet under the highest SLR scenario. Magnitude and direction of maximum velocities can be determinant for inlet formation and stability in multiple inlet systems (Friedrichs et al., 1993; Salles et al., 2005); moreover, changes in maximum velocities can also impact sediment transport and sedimentation patterns, which could cause bathymetric changes in the lagoon (Dronkers, 1986; Ashley, 1988). The velocity changes observed under SLR, in conjunction with the changes in tidal parameters (tidal asymmetry), show that it is reasonable to expect bathymetric changes derived from the impact of SLR in the Ria Formosa hydrodynamics.

Four SLR scenarios were chosen from literature and simulated to study the impact of SLR in the hydrodynamics of the Ria Formosa; the selection of SLR values was based on covering a wide range of SLR intensity (0.47 m to 0.84 m in the year 2100) to better characterize the response of the system to SLR. The results of the study seem to suggest a proportional relationship over time between the intensity of SLR and the strength in the response of the system; this is likely a consequence of implementing SLR as a relatively linear rate in the simulations. It is more likely that SLR will start small in the short-term future, and future contributors (e.g. melting of the Antarctic and Greenland ice sheets, thermal expansion; Church and White, 2006; Rignot, 2011) will accelerate SLR at the end of the century.

## 6.2. Long term morphological evolution of the Ria Formosa

To simulate the long-term morphological changes in the Ramalhete Channel and the neighbouring areas, a structured model approach was used to evaluate SLR impacts in local bathymetry changes, sediment transport and channel displacement. The structured model results showed the highest bathymetric changes in the inlets' areas, with several patches of accretion and erosion exceeding values of 2 m (Figures 6.3 and 6.4). However, it must be noted that the model was tuned to analyse morphological changes inside of the lagoon, and that the lack of coupled wave-modelling and calibration and validation processes reduces the reliability of the predictions of morphological changes in the inlets.

The impact of the applied SLR (as a linear rate of 1.1 mm/yr) in the bathymetry of the Ramalhete Channel and its margins appears to be relatively small, with erosion values of ~0.1

m after the 89 years of simulation. No channel displacements were observed. The recorded bathymetric changes are slightly higher in the salt marsh area: overall, erosion prevails over accretion, with some patches of erosion reaching values in the range of 0.1 to 0.3 m, suggesting an unbalanced sediment built-up within SLR. The strong accretion patches are likely a miscalculation of the model, as over 2 m of accretion appear in the last period of simulation (75 to 89 years) with no significant bathymetric changes seen in the surrounding areas of the patches. Erosion values seen under the SLR scenario (RCP8.5) might imply negative future consequences for salt marshes under SLR. Salt marshes reduce water flow and facilitate sedimentation, but this accretion appears to be limited to a specific tidal range between Mean Water Level and Mean High Water Level (Orson et al., 1985; Neumeier and Ciavola, 2004; Bartholdy et al., 2004). Although our results do not show clear impacts of SLR in salt marsh morphodynamics, salt marshes could be negatively affected by SLR through sediment concentration. The capacity of salt marshes to adapt to SLR is greatly reduced when sediment concentrations are low (Mariotti and Fagherazzi, 2010), which could potentially endanger them once SLR increases after a certain threshold. In this study a SLR rate of 1.1 mm/year was simulated, smaller than those reported as manageable by salt marshes by different authors (Bartholdy et al., 2004; Bartholdy et al., 2010; Mariotti and Fagherazzi, 2010); this suggests that salt marshes might be able to adjust to SLR without negative consequences for the ecological equilibrium of the lagoon. However, this cannot be stated without further research to determine survivable RSLR rates in salt marshes of the Ria Formosa.

In the remaining channels, bathymetric change rates under SLR were generally low for all cross-sections and all timesteps simulated except for Cs16 (located in the Ancão Channel; Table 6.1) in the latest timesteps. Paired with the expected increase in water elevation caused by SLR, the obtained results suggest that under SLR the channel will deepen, which could be a sign of changes in local hydrodynamic processes. Strong residual flow circulation has been reported in the Ria Formosa and has been suggested to play an important role in producing net landward or seaward sediment transport (Salles et al., 2005; Dias et al., 2009). Furthermore, Valentim et al. (2013) studied the impact of SLR in residual circulation in the Tagus estuary and reported a significant decrease in the residual circulation of the estuary, albeit a slight increase in residual circulation was found in some areas of the estuary mouth. This is in agreement with the findings of Carrasco et al. (2018), who studied tide circulation patterns under SLR in the Ria Formosa and proposed that under the most likely future scenario for the coastal lagoon (a basin-infilling scenario) changes in net transport sediment will alter lagoon sedimentation feedbacks.

The predicted hydrodynamic and morphological changes due to SLR in the next 89 years for the Ria Formosa lagoon are not massive, though some social, economic and ecological consequences can be derived, including but not limited, interference with the natural resources, increase in flood of intertidal areas, and, lately, interference with current habitats and ecosystems functioning (Bilskie et al., 2014; Prime et al., 2015; Carrasco et al., 2016; Vousdouskas et al., 2017). No major economic changes are foreseen for the bivalve farming, as no major bathymetric changes in marshes and channel margins are expected to occur. Nevertheless, the predicted changes in tidal asymmetry might carry some physical adjustments in the farming constructions in the future.

## 6.3 Limitations of the study

In this study two model approaches were used: an unstructured model approach using Delft3D-Flexible Mesh to simulate hydrodynamic changes in the system, and a structured approach using Delft3D-Flow with morphodynamic updating to simulate morphodynamic changes in the system. The results showed certain limitations of the study, that should be noted and improved in future research.

The unstructured approach was calibrated and validated using water levels and velocity currents; however, there is still a need to collect quality hydrodynamic data for more thorough calibration and validation processes. In the preparation stages of the structured grid model setup, some variables (grid refinement, mean sediment size, bottom roughness coefficient Morfac) of the calibrated and validated model by González-Gorbeña et al (2018) were altered, to increase the accuracy and efficiency of the modelling processes based on scientific knowledge of the system. The resolution of the curvilinear grid used in the structured model approach was not optimal, with a coarse refinement applied to a wide area of interest (from the entrance of the Olhão Channel to the westernmost area of the Ria Formosa). No further calibration or validation processes were applied to the model, which introduces a degree of uncertainty to the model results that must be noted.

The low elevation differences found inside of the lagoon suggest an imbalance in sediment input and very low sediment transport. Although differences in sediment transport values are expected within the lagoon, sediment transport and morphological changes should be seen in inner areas like the Ramalhete Channel. This is supported by the modelling results of van der Wegen (2013) and Dissanayake et al. (2015), who reported an increase in sediment import and landward-sediment transport in estuaries under SLR.

Several factors could have induced low sediment transport values. The lack of accurate information regarding grain size distribution over the study area contributed to modelling uncertainties; therefore, collection and analysis of sediment samples in the Faro, Ramalhete and Armona channels will provide useful information for future modelling studies in the Ria Formosa lagoon. Another challenge was to include an additional external sediment supply. Coastal lagoon sediments are mixtures of sediments from various sources (Nicholls and Boon, 1994) and their sizes in the Ria Formosa vary from mud (<0.064 μm) to medium sand (0.25 - 0.5 μm; González-Gorbeña, 2018; Carrasco et al., 2019). In the present study a median grain size of 175 μm was used, as that was the main sediment size coming through the main source of sediment in the lagoon, the Faro-Olhão Inlet (Carrasco et al., 2019). This simplification reduced sediment transport throughout the lagoon, which limits the capacity of the model to assess the effect of SLR in inner areas of the lagoon (tidal channels, tidal flats, salt marshes). For the present model, the modelling of just another sediment fraction doubled simulation time; however, future studies should consider finding a way to model more fractions of sediments to better represent sediment transport throughout the Ria Formosa coastal lagoon.

The effect of waves was not simulated in this study for the sake of simplicity. Bathymetric changes under SLR in the inlets were not considered reliable, due to waves being one of the main factors affecting inlet morphology. Although Plecha et al. (2010) reported that waves were not necessary to optimize modelled morphological evolution within the Ria de Aveiro tidal inlet (despite a highly energetic wave climate), the present results imply that waves are a necessary inclusion when modelling the morphological evolution of the Ria Formosa under SLR. As an approximation to increase SLR, this study applied a linear water level increase for the SLR scenario. Although the final SLR value for 2100 (0.98 m) coincides with the final predicted SLR, this linear trend is not in agreement with the RCP 8.5 reported by the IPCC (2014; 2019). The RCP 8.5 scenario predicts a slower pace of SLR acceleration for the first 50 years and a faster pace from 2050 to 2100 (IPCC, 2014; 2019). Therefore, morphological evolution should be relatively low up to 2050 and show further acceleration afterwards. The results of this study show this pattern, with the highest bathymetric change rates appearing in the second half of the simulation time (Table 6.1); however, a direct implementation of SLR trends would provide more reliable data on morphological evolution of the Ria Formosa lagoon.

Finally, to improve our understanding of the Ria Formosa coastal lagoon, some suggestions for future additions to the present model are:

-To optimize model settings by applying bed roughness in more detail, improving the grid resolution and representing vegetation throughout the lagoon.

-To improve sediment input representation by adding external sediment sources, more sediment fractions and cohesive sediments.

-To include additional forcing processes, such as the effect of wind or the effect of waves at the inlets.

# Chapter 7: Conclusions

This study evaluates the effects of SLR in the hydrodynamic processes of the Ria Formosa and provides a first modelling approach to simulate the effects of SLR in the morphodynamic processes of the lagoon. A two-dimensional, process-based approach was utilized in this study, with (1) an unstructured grid and several SLR rates simulated to explore the hydrodynamic processes, and (2) a structured grid with one rate of SLR to explore the morphodynamic processes; the unstructured model did not include at the time a morphological module. The unstructured model was calibrated and validated with historical water level and current velocity data. After the calibration process the setup with lowest accumulated RMSE was selected for validation. Excellent skill was found for three out four of the data arrays, with the other one showing good skill. Four SLR rates were applied in this study as an additional tidal constituent of the astronomical boundary. A certain degree of uncertainty in the results of the structured approach is to be expected due to the selected grid setup, lack of calibration and validation and absence of waves; nevertheless, this study provides insight into the effects of SLR in the morphodynamic processes of coastal lagoons. A SLR of 0.98 m (~1.1 mm/year) was applied to the structured model as an additional boundary component.

Strength and type of tidal asymmetry and average and maximum current velocities were analysed. Under SLR tidal asymmetry strength generally decreased within the lagoon and increased under the influence of specific local bathymetry characteristics. SLR progressively enhanced flood-dominance in the lagoon due to an increase in the influence of the Ancão Inlet. Changes in tidal prism exchanges through the inlets are expected, specifically an increase in the tidal prism captured by the Ancão Inlet and a decrease in tidal prism captured by the Faro-Olhão and Armona inlets. Maximum velocities in the cross-sections modelled in the Faro Channel show a shift of the period in which maximum velocities occur, from flood to ebb. These results imply that bathymetric changes will be derived from the effect of SLR in the hydrodynamic processes of the Ria Formosa.

Bathymetric changes in the western sector of the Ria Formosa and in the Ramalhete Channel and cross-sectional bathymetry profiles along the Faro, Ramalhete and Ancão channels were analysed. Erosion ranging from 0.1 to 0.3m was found under SLR in the salt marsh area between the channels. One of the cross-sectional bathymetry profiles (Cs16) located in the Ancão Channel showed erosion of 0.3 m in the bottom of the channel and accretion of 0.2 m in the channel margins. SLR-induced changes in residual flow might explain these bathymetric changes and hint that changes in hydrodynamic processes caused by SLR will cause bathymetric changes. The results overall hint that no major economic or ecological impact is expected from the impacts of SLR in the Ria Formosa.

Despite some limitations, the results of this study contribute to the scientific knowledge about the effect of SLR in the hydrodynamics of coastal lagoons, provide an assessment of the possible morphological, economic and ecological impacts of SLR in the Ria Formosa and provide suggestions for future studies regarding the effect of SLR in the morphodynamic processes of coastal lagoons.

# References


Anthony, A., Atwood, J., August, P., Byron, C., Cobb, S., Foster, C., ... & Kellogg, D. Q. (2009). Coastal lagoons and climate change: ecological and social ramifications in US Atlantic and Gulf coast ecosystems. Ecology and Society, 14(1).

Antunes, C., & Taborda, R. (2009). Sea level at Cascais tide gauge: data, analysis and results. *Journal of Coastal Research*, 218-222.

Agência Portuguesa do Ambiente. (2017). *Diagnóstico do setor da produção ostreícola na Ria Formosa*. Ministério do Ambiente e Ação Climática. https://apambiente.pt/_zdata/Divulgacao/Publicacoes/Guias%20e%20Manuais/Relatorio_Ria_Formosa_Ostreicultura.pdf

Ashley, G. M., & Grizzle, R. E. (1988). Interactions between hydrodynamics, benthos and sedimentation in a tide-dominated coastal lagoon. *Marine Geology*, *82*(1-2), 61-81.

Aubrey, D. G., & Speer, P. E. (1985). A study of non-linear tidal propagation in shallow inlet/estuarine systems Part I: Observations. *Estuarine, Coastal and Shelf Science*, *21*(2), 185-205.

Bartholdy, J., Christiansen, C., & Kunzendorf, H. (2004). Long term variations in backbarrier salt marsh deposition on the Skallingen peninsula–the Danish Wadden Sea. *Marine Geology*, *203*(1-2), 1-21.

Bartholdy, A. T., Bartholdy, J., & Kroon, A. (2010). Salt marsh stability and patterns of sedimentation across a backbarrier platform. *Marine Geology*, *278*(1-4), 31-42.

Bettencourt, P. (1994). *Les Environnements sédimentaires de la côte sotavento (Algarve, Sud Portugal) et leur évolution holocène et actuelle. Bordeaux: Université Bordeaux I* (Doctoral dissertation, thèse de doctorat, spécialité Géologie marine). In French.

Bilskie, M. V., Hagen, S. C., Medeiros, S. C., & Passeri, D. L. (2014). Dynamics of sea level rise and coastal flooding on a changing landscape. *Geophysical Research Letters*, *41*(3), 927-934.

Carrasco, A. R., Ferreira, O., & Roelvink, D. (2016). Coastal lagoons and rising sea level: A review. *Earth-Science Reviews, 154*, 356–368. https://doi.org/10.1016/j.earscirev.2015.11.007

Carrasco, A. R., Plomaritis, T., Reyns, J., Ferreira, Ó., & Roelvink, D. (2018). Tide circulation patterns in a coastal lagoon under sea-level rise. *Ocean Dynamics*, 68(9), 1121-1139.

Carrasco, R., van den Hoven, K., Ferreira, Ó. (2019). Modelling morphological impact of SLR on the Ria Formosa lagoon. CIMA – Universidade do Algarve. 8pp. Retrieved from: http://evrest.cvtavira.pt/wpcontent/uploads/2019/10/EVREST_Modelling_Report09_2019.pdf

Church, J. A., & White, N. J. (2006). A 20th century acceleration in global sea-level rise. *Geophysical research letters*, *33*(1).

Coco, G., Zhou, Z., Van Maanen, B., Olabarrieta, M., Tinoco, R., & Townend, I. (2013). Morphodynamics of tidal networks: advances and challenges. *Marine Geology, 346*, 1-16.

Costa, M., Silva, R., & Vitorino, J. (2001). Contribuição para o estudo do clima de agitação marítima na costa portuguesa. *2ª Jornadas Portuguesas de Engenharia Costeira e Portuária*, 20. In Portuguese.

Cravo, A., Cardeira, S., Pereira, C., Rosa, M., Madureira, M., Rita, F., ... & Jacob, J. (2013). Nutrients and particulate matter exchanges through the Ria Formosa coastal lagoon, Portugal. *Journal of Coastal Research,* (65), 1999-2004.

Cronin, T. M. (2012). Rapid sea-level rise. *Quaternary Science Reviews, 56*, 11-30.

Defina, A., Carniello, L., Fagherazzi, S., & D'Alpaos, L. (2007). Self-organization of shallow basins in tidal flats and salt marshes. *Journal of Geophysical Research: Earth Surface, 112*(F3).

Deltares systems. (2014). *Delft3D-FLOW, User Manual*, 1–684. Retrieved from www.deltaressystems.nl

Dias, J. M., & Sousa, M. C. (2009). Numerical modeling of Ria Formosa tidal dynamics. *Journal of Coastal Research, 2009* (56), 1345–1349.

Dias, J. M., Sousa, M. C., Bertin, X., Fortunato, A. B., & Oliveira, A. (2009). Numerical modeling of the impact of the Ancão Inlet relocation (Ria Formosa, Portugal). *Environmental Modelling and Software, 24*(6).

Dissanayake, D. M. P. K., Ranasinghe, R. W. M. R. J. B., & Roelvink, J. A. (2012). The morphological response of large tidal inlet/basin systems to relative sea level rise. *Climatic change, 113*(2), 253-276.

Dissanayake, P., Karunarathna, H., & Ranasinghe, R. (2015). Numerical modelling of the impact of sea level rise on large tidal inlet/basin systems. In *36th IAHR World Congress 2015: Delta's of the future (and what hapens upstream)*. IAHR.

Dronkers, J. (1986). Tidal asymmetry and estuarine morphology. *Netherlands Journal of Sea Research*, *20*(2-3), 117-131.

Duarte, P., Azevedo, B., Guerreiro, M., Ribeiro, C., Bandeira, R., Pereira, A., ... & Reia, J. (2008). Biogeochemical modelling of Ria Formosa (South Portugal). *Hydrobiologia, 611*(1), 115-132.

Edwards, R. J. (2007). Low Energy Coasts Sedimentary Indicators. *Encyclopedia of Quaternary Sciences. Elsevier, London, UK*, 2994-3006.

Egbert, G. D., Bennett, A. F., & Foreman, M. G. (1994). TOPEX/POSEIDON tides estimated using a global inverse model. *Journal of Geophysical Research: Oceans, 99*(C12), 24821-24852.

Egbert, G. D., & Erofeeva, S. Y. (2002). Efficient inverse modeling of barotropic ocean tides. Journal of Atmospheric and Oceanic Technology, *19*(2), 183-204.

Fitzgerald, D. M., Penland, S., & Nummedal, D. A. G. (1984). Control of barrier island shape by inlet sediment bypassing: East Frisian Islands, West Germany. *Marine Geology, 60*(1-4), 355-37

Fitzgerald, D. F., Buynevich, I., & Argow, B. (2006). Model of tidal inlet and barrier island dynamics in a regime of accelerated sea level rise. *Journal of Coastal Research,* 789-795.

Fortunato, A. B., & Oliveira, A. (2005). Influence of intertidal flats on tidal asymmetry. *Journal of*

*Coastal Research*, *21*(5 (215)), 1062-1067.

Friedrichs, C. T., Aubrey, D. G., & Speer, P. E. (1990). Impacts of relative sea-level rise on evolution of shallow estuaries. In *Residual currents and long-term transport* (pp. 105-122). Springer New York.

Friedrichs, C. T., Aubrey, D. G., Giese, G. S., & Speer, P. E. (1993). Hydrodynamical modeling of a multiple-inlet estuary/barrier system: insight into tidal inlet formation and stability. *Coastal and Estuarine Studies*, 95-95.

Friedrichs, C. T., & Aubrey, D. G. (1994). Tidal propagation in strongly convergent channels. *Journal of Geophysical Research: Oceans*, *99*(C2), 3321-3336.

Gillanders, B. M., Elsdon, T. S., Halliday, I. A., Jenkins, G. P., Robins, J. B., & Valesini, F. J. (2011). Potential effects of climate change on Australian estuaries and fish utilising estuaries: a review. *Marine and Freshwater Research*, *62*(9), 1115-1131.

González-Gorbeña, E., Pacheco, A., Plomaritis, T. A., Ferreira, Ó., & Sequeira, C. (2018). Estimating the optimum size of a tidal array at a multi-inlet system considering environmental and performance constraints. *Applied Energy*, *232*, 292-311.

Guo, L., Van der Wegen, M., Roelvink, J. A., & He, Q. (2014). The role of river flow and tidal asymmetry on 1-D estuarine morphodynamics. *Journal of Geophysical Research: Earth Surface*, *119*(11), 2315-2334.

IPCC (2014) Climate change 2014: mitigation of climate change. In: Edenhofer O, Pichs-Madruga R, Sokona Y, Farahani E, Kadner S, Seyboth K, Adler A, Baum I, Brunner S, Eickemeier P, Kriemann B, Savolainen J, Schlömer S, von Stechow C, Zwickel T, Minx JC (eds) Contribution of Working Group III to the Fifth Assessment Report of the Intergovernmental Panel on Climate Change. Cambridge University. Press, Cambridge

IPCC (2019). Hoegh-Guldberg, O., D. Jacob, M. Taylor, M. Bindi, S. Brown, I. Camilloni, A. Diedhiou, R. Djalante, K.L. Ebi, F. Engelbrecht, J. Guiot, Y. Hijioka, S. Mehrotra, A. Payne, S.I. Seneviratne, A. Thomas, R. Warren, and G. Zhou, 2018: Impacts of 1.5ºC Global Warming on Natural and Human Systems. In: Global Warming of 1.5°C. An IPCC Special Report on the impacts of global warming of 1.5°C above pre-industrial levels and related global greenhouse gas emission pathways, in the context of strengthening the global response to the threat of climate change, sustainable development, and efforts to eradicate poverty [Masson-Delmotte, V., P. Zhai, H.-O. Pörtner, D. Roberts, J. Skea, P.R. Shukla, A. Pirani, W. Moufouma-Okia, C. Péan, R. Pidcock, S. Connors, J.B.R. Matthews, Y. Chen, X. Zhou, M.I. Gomis, E. Lonnoy, T. Maycock, M. Tignor, and T. Waterfield (eds.)]. In Press

Jacob, J., Cardeira, S., Rodrigues, M., Bruneau, N., Azevedo, A., Fortunato, A. B., ... & Cravo, A. (2013). Experimental and numerical study of the hydrodynamics of the western sector of Ria Formosa. *Journal of Coastal Research*, *65*(sp2), 2011-2016.

Jacob, J., & Cravo, A. (2019). Recent evolution of the tidal prisms at the inlets of the western sector of

the Ria Formosa, south coast of Portugal. *Regional Studies in Marine Science, 31*, 100767.

Jackson, L. P., & Jevrejeva, S. (2016). A probabilistic approach to 21st century regional sea-level projections using RCP and high-end scenarios. *Global and Planetary Change, 146*, 179-189.

Kernkamp, H. W., Van Dam, A., Stelling, G. S., & de Goede, E. D. (2011). Efficient scheme for the shallow water equations on unstructured grids with application to the Continental Shelf. *Ocean Dynamics, 61*(8), 1175-1188.

Kirwan, M. L., & Murray, A. B. (2008). Ecological and morphological response of brackish tidal marshland to the next century of sea level rise: Westham Island, British Columbia. *Global and Planetary Change, 60*(3), 471-486.

Kjerfve, B. (1994). Coastal lagoons. In Elsevier oceanography series (Vol. 60, pp. 1-8). Elsevier.

Kombiadou, K., Matias, A., Ferreira, Ó., Carrasco, A. R., Costas, S., & Plomaritis, T. (2019). Impacts of human interventions on the evolution of the Ria Formosa barrier island system (S. Portugal). *Geomorphology, 343*, 129-144.

Lesser, G. R., Roelvink, J. V., Van Kester, J. A. T. M., & Stelling, G. S. (2004). Development and validation of a three-dimensional morphological model. Coastal engineering, *51*(8-9), 883-915.

Lesser, G. R. (2009). *An approach to medium-term coastal morphological modelling*. IHE Delft Institute for Water Education.

List, J. H., Sallenger, A. H., Hansen, M. E., & Jaffe, B. E. (1997). Accelerated relative sea-level rise and rapid coastal erosion: testing a causal relationship for the Louisiana barrier islands. *Marine geology, 140*(3), 347-365.

Lopes, C. L., Silva, P. A., Dias, J. M., Rocha, A., Picado, A., Plecha, S., & Fortunato, A. B. (2011). Local sea level change scenarios for the end of the 21st century and potential physical impacts in the lower ria de aveiro (Portugal). *Continental Shelf Research, 31*(14), 1515–1526. https://doi.org/10.1016/j.csr.2011.06.015

Louters, T., Gerritsen, F., & Essink, K. (1994). *The riddle of the sands: a tidal system's answer to a rising sea level*. Ministry of Transport, Public Works and Water Management, Directorate-General of Public Works and Water Management, National Institute for Coastal and Marine Management (RIKZ).

Mariotti, G., & Fagherazzi, S. (2010). A numerical model for the coupled long‐term evolution of salt marshes and tidal flats. *Journal of Geophysical Research: Earth Surface, 115*(F1).

Martin, L., & Dominguez, J. M. L. (1994). Geological history of coastal lagoons. In Elsevier *Oceanography Series* (Vol. 60, pp. 41-68). Elsevier.

Moore, L. J., List, J. H., Williams, S. J., & Stolper, D. (2010). Complexities in barrier island response to sea level rise: Insights from numerical model experiments, North Carolina Outer Banks. *Journal of Geophysical Research: Earth Surface, 115*(F3).

Neumeier, U., & Ciavola, P. (2004). Flow resistance and associated sedimentary processes in a

Spartina maritima salt-marsh. *Journal of Coastal Research*, 20(2 (202)), 435-447.

Nichols, M. M., & Boon, J. D. (1994). Sediment transport processes in coastal lagoons. In Elsevier oceanography series (Vol. 60, pp. 157-219). Elsevier.

Nicholls, R. J. (2004). Coastal flooding and wetland loss in the 21st century: Changes under the SRES climate and socio-economic scenarios. *Global Environmental Change, 14*(1), 69–86.

Nichols, M. M., & Boon, J. D. (1994). Sediment transport processes in coastal lagoons. In *Elsevier oceanography series* (Vol. 60, pp. 157-219). Elsevier.

Nicholls, R. J., Hanson, S. E., Lowe, J. A., Warrick, R. A., Lu, X., & Long, A. J. (2014). Sea-level scenarios for evaluating coastal impacts. *Wiley Interdisciplinary Reviews: Climate Change*, *5*(1), 129–150.

Orson, R., Panageotou, W., & Leatherman, S. P. (1985). Response of tidal salt marshes of the US Atlantic and Gulf coasts to rising sea levels. *Journal of Coastal Research*, 29-37.

Pacheco, A., Vila-Concejo, A., Ferreira, Ó., & Dias, J. A. (2008). Assessment of tidal inlet evolution and stability using sediment budget computations and hydraulic parameter analysis. *Marine Geology, 247*(1), 104-127.

Pacheco, A., Ferreira, Ó., Williams, J. J., Garel, E., Vila-Concejo, A., & Dias, J. A. (2010). Hydrodynamics and equilibrium of a multiple-inlet system. *Marine Geology, 274*(1–4), 32–42. https://doi.org/10.1016/j.margeo.2010.03.003

Pacheco, A., Williams, J. J., Ferreira, Ó., Garel, E., & Reynolds, S. (2011). Application of sediment transport models to a multiple-inlet system. estuarine. *Coastal and Shelf Science, 95*, 119-134.

Pawlowicz, R., Beardsley, B., & Lentz, S. (2002). Classical tidal harmonic analysis including error estimates in MATLAB using T_TIDE. *Computers & Geosciences*, *28*(8), 929-937.

Pendleton, E. A., & FitzGerald, D. M. (2005). Comparison of the hydrodynamic character of three tidal inlet systems. *High Resolution Morphodynamics and Sedimentary Evolution of Estuaries*, 83-100.

Plecha, S., Silva, P. A., Vaz, N., Bertin, X., Oliveira, A., Fortunato, A. B., & Dias, J. M. (2010). Sensitivity analysis of a morphodynamic modelling system applied to a coastal lagoon inlet. *Ocean Dynamics*, *60*(2), 275-284.

Prime, T., Brown, J. M., & Plater, A. J. (2015). Physical and economic impacts of sea-level rise and low probability flooding events on coastal communities. *PLoS One*, *10*(2), e0117030.

Rosa, A., Cardeira, S., Pereira, C., Rosa, M., Madureira, M., Rita, F., ... & Cravo, A. (2019). Temporal variability of the mass exchanges between the main inlet of Ria Formosa lagoon (southwestern Iberia) and the Atlantic Ocean. Estuarine, *Coastal and Shelf Science*, *228*, 106349.

Rizzetto, F., & Tosi, L. (2012). Rapid response of tidal channel networks to sea-level variations (Venice Lagoon, Italy). *Global and Planetary Change, 92*, 191-197.

Salles, P. (2001). Hydrodynamic controls on multiple tidal inlet persistence (Doctoral dissertation,

Massachusetts Institute of Technology and Woods Hole Oceanographic Institution).

Salles, P., Voulgaris, G., & Aubrey, D. G. (2005). Contribution of nonlinear mechanisms in the persistence of multiple tidal inlet systems. *Estuarine, Coastal and Shelf Science, 65*(3), 475–491. https://doi.org/10.1016/j.ecss.2005.06.018

Slangen, A. B. A., Katsman, C. A., Van de Wal, R. S. W., Vermeersen, L. L. A., & Riva, R. E. M. (2012). Towards regional projections of twenty-first century sea-level change based on IPCC SRES scenarios. *Climate dynamics*, 38(5-6), 1191-1209.

Sousa, C., Boski, T., & Pereira, L. (2019). Holocene evolution of a barrier island system, Ria Formosa, South Portugal. *The Holocene*, *29*(1), 64-76.

Stefanon, L., Carniello, L., D'Alpaos, A., & Rinaldo, A. (2012). Signatures of sea level changes on tidal geomorphology: Experiments on network incision and retreat. *Geophysical Research Letters*, 39(12).

Stark, J., Smolders, S., Meire, P., & Temmerman, S. (2017). Impact of intertidal area characteristics on estuarine tidal hydrodynamics: A modelling study for the Scheldt Estuary. *Estuarine, Coastal and Shelf Science*, *198*, 138-155.

Storms, J. E., Weltje, G. J., Van Dijke, J. J., Geel, C. R., & Kroonenberg, S. B. (2002). Process-response modeling of wave-dominated coastal systems: simulating evolution and stratigraphy on geological timescales. *Journal of sedimentary Research*, *72*(2), 226-239.

Valentim, J. M., Vaz, L., Vaz, N., Silva, H., Duarte, B., Caçador, I., & Dias, J. M. (2013). Sea level rise impact in residual circulation in Tagus estuary and Ria de Aveiro lagoon. *Journal of Coastal Research*, (65), 1981-1986.

van der Wegen, M. (2013). Numerical modeling of the impact of sea level rise on tidal basin morphodynamics. *Journal of Geophysical Research: Earth Surface*, *118*(2), 447-460.

van Goor, M. A., Zitman, T. J., Wang, Z. B., & Stive, M. J. F. (2003). Impact of sea-level rise on the morphological equilibrium state of tidal inlets. *Marine Geology*, *202*(3–4), 211–227.

Vila-Concejo, A., Ferreira, Ó., Morris, B. D., Matias, A., & Dias, J. M. A. (2004). Lessons from inlet relocation: Examples from Southern Portugal. *Coastal Engineering*, *51*(10), 967–990.

Vousdouskas, M. I., Mentaschi, L., Voukouvalas, E., Verlaan, M., & Feyen, L. (2017). Extreme sea levels on the rise along Europe's coasts. *Earth's Future*, *5*(3), 304-323.

Walters, D., Moore, L. J., Duran Vinent, O., Fagherazzi, S., & Mariotti, G. (2014). Interactions between barrier islands and backbarrier marshes affect island system response to sea level rise: Insights from a coupled model. *Journal of Geophysical Research: Earth Surface*, *119*(9), 2013-2031.

Zhang, K., Douglas, B. C., & Leatherman, S. P. (2004). Global warming and coastal erosion. *Climatic Change*, *64*(1), 41-58.

# I ANNEX

Table I.1. Bathymetric exchange rates in mm/yr for all cross-sections. Cross-sections without changes at any point are left out.

| | Baseline scenario | | | | | SLR scenario | | | | |
|---|---|---|---|---|---|---|---|---|---|---|
| **Cross section** | **0-25 years** | **25-50 years** | **50-75 years** | **75-89 years** | **0-89 years** | **0-25 years** | **25-50 years** | **50-75 years** | **75-89 years** | **0-89 years** |
| **1** | 0.30 | 0.15 | 0.04 | 0.01 | 0.05 | 0.17 | 0.01 | -0.01 | 6.08E-04 | 0.14 |
| **6** | 0 | 0 | 0 | 0 | 1.16E-07 | 0 | 0 | 2.07E-07 | 3.69E-07 | 0 |
| **7** | 3.27E-06 | 2.25E-05 | 0 | 0 | 3.93E-05 | 3.23E-08 | 4.39E-06 | 6.79E-05 | 1.21E-04 | 7.22E-06 |
| **8** | 0 | 0 | 0 | 0 | 2.68E-05 | 2.89E-08 | 1.17E-05 | 4.78E-05 | 6.42E-05 | 0 |
| **9** | 0 | -1.78E-14 | 0 | -3.17E-14 | 1.71E-05 | 3.55E-14 | 2.80E-10 | 4.23E-05 | 3.35E-05 | -9.98E-15 |
| **10** | 0 | 0 | 0 | 0 | 5.71E-06 | 0 | 1.79E-07 | 1.03E-05 | 1.76E-05 | 0 |
| **11** | 1.23E-11 | 1.15E-11 | 1.15E-11 | 1.16E-11 | 1.66E-05 | 6.06E-08 | 4.49E-08 | 6.36E-06 | 9.37E-05 | 1.18E-11 |
| **13** | 4.06E-11 | 3.21E-11 | 2.93E-11 | 3.12E-11 | -9.27E-11 | 1.24E-11 | -1.53E-10 | -9.44E-11 | -1.69E-10 | 3.36E-11 |
| **14** | -9.88E-12 | -9.70E-12 | -9.73E-12 | -8.72E-12 | 2.42E-05 | -2.81E-12 | 2.15E-11 | 5.99E-10 | 1.5E-04 | -9.61E-12 |
| **15** | 7.11E-13 | 7.11E-13 | 6.75E-13 | 6.66E-13 | 0.08 | 6.22E-13 | 4.92E-4 | 0.07 | 0.41 | 6.94E-13 |
| **16** | 0.01 | 8.40E-4 | 1.882387E-3 | 1.05E3 | -3.44 | 0.04 | 0.56 | 19.4 | -57.5 | 2.97E-03 |

Figure I.1. Channel bathymetry (upper graph) and elevation differences between scenarios (lower graph) in Cs1-5. Positive values in elevation differences indicate accretion and negative values indicate erosion.

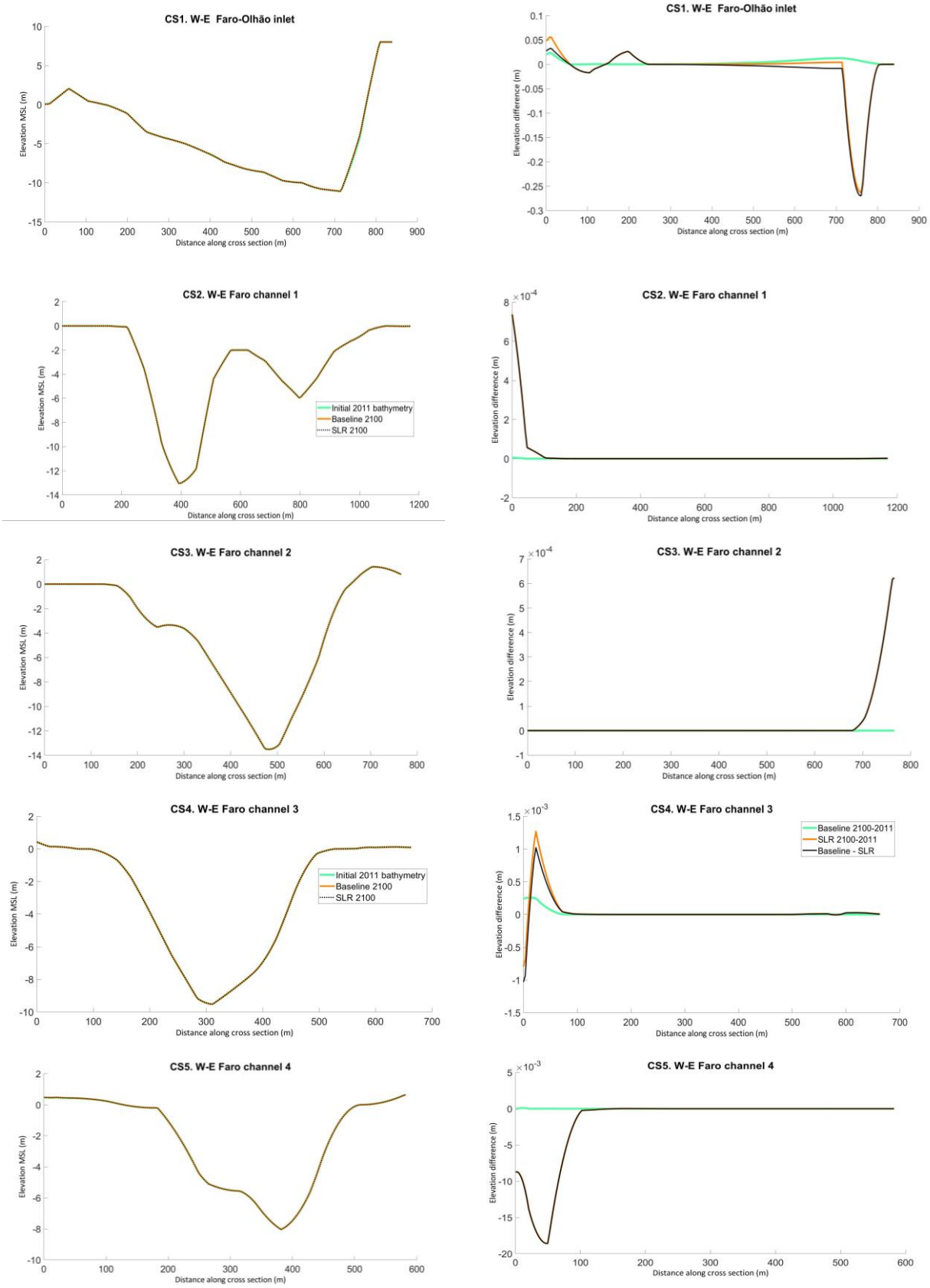

Figure I.2. Channel bathymetry (upper graph) and elevation differences between scenarios (lower graph) in Cs6-10. Positive values in elevation differences indicate accretion and negative values indicate erosion.

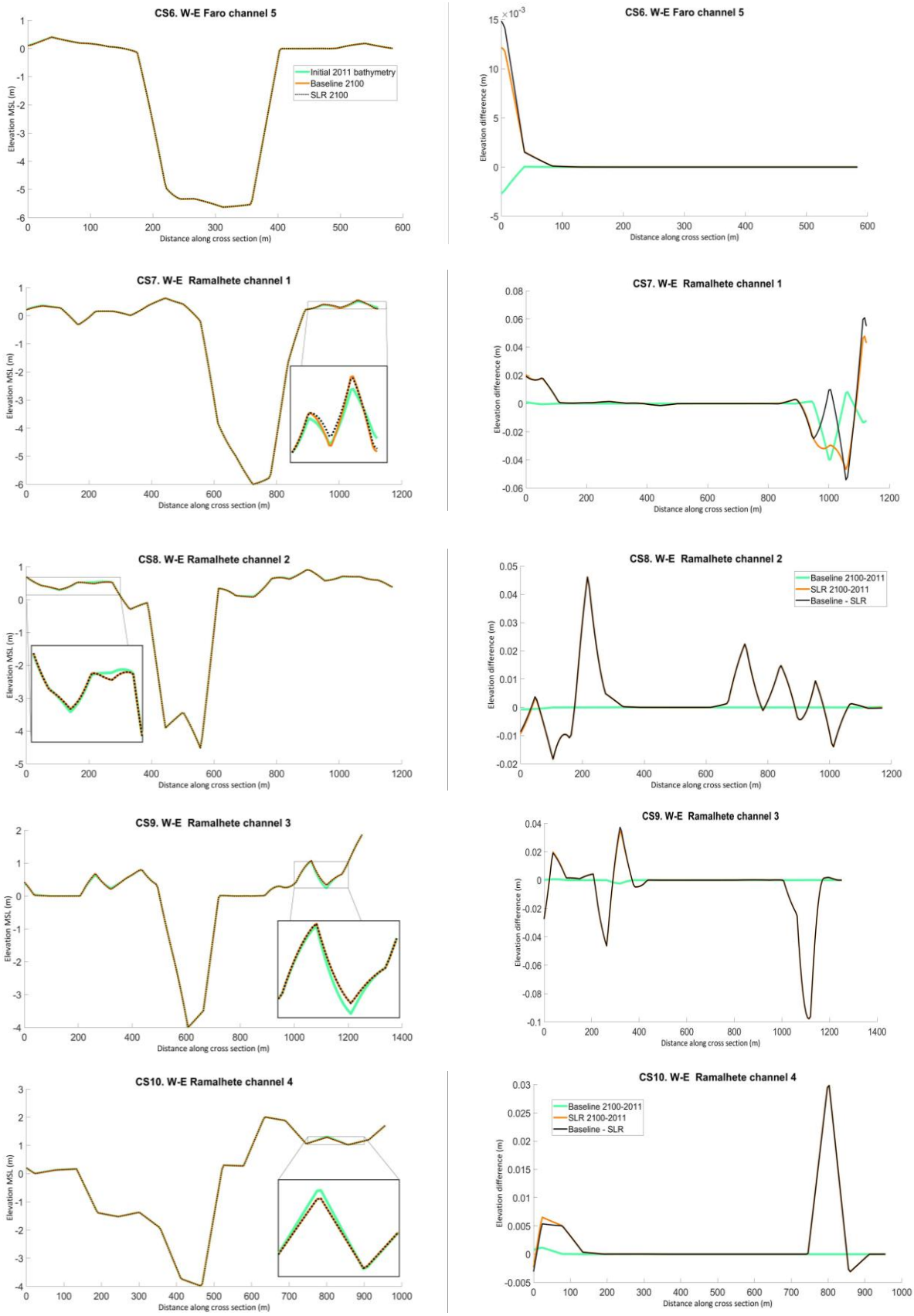

Figure I.3. Channel bathymetry (upper graph) and elevation differences between scenarios (lower graph) in Cs11-15. Positive values in elevation differences indicate accretion and negative values indicate erosion.